2017

Laboratory Performance Comparison of Vortecone Inertial Dust Scrubber to Flooded-Bed Dust Scrubber

Adam J. Levy
University of Kentucky, adam.levy201@gmail.com
Digital Object Identifier: https://doi.org/10.13023/ETD.2017.106

STUDENT AGREEMENT:

I represent that my thesis or dissertation and abstract are my original work. Proper attribution has been given to all outside sources. I understand that I am solely responsible for obtaining any needed copyright permissions. I have obtained needed written permission statement(s) from the owner(s) of each third-party copyrighted matter to be included in my work, allowing electronic distribution (if such use is not permitted by the fair use doctrine) which will be submitted to UKnowledge as Additional File.

I hereby grant to The University of Kentucky and its agents the irrevocable, non-exclusive, and royalty-free license to archive and make accessible my work in whole or in part in all forms of media, now or hereafter known. I agree that the document mentioned above may be made available immediately for worldwide access unless an embargo applies.

I retain all other ownership rights to the copyright of my work. I also retain the right to use in future works (such as articles or books) all or part of my work. I understand that I am free to register the copyright to my work.

REVIEW, APPROVAL AND ACCEPTANCE

The document mentioned above has been reviewed and accepted by the student's advisor, on behalf of the advisory committee, and by the Director of Graduate Studies (DGS), on behalf of the program; we verify that this is the final, approved version of the student's thesis including all changes required by the advisory committee. The undersigned agree to abide by the statements above.

Adam J. Levy, Student

Dr. William C. Wedding, Major Professor

Dr. Zach Agioutantis, Director of Graduate Studies

LABORATORY PERFORMANCE COMPARISON OF VORTECONE INERTIAL DUST SCRUBBER TO FLOODED-BED DUST SCRUBBER

THESIS

A thesis submitted in partial fulfillment of the requirements for the degree of Master of Science in Mining Engineering in the College of Engineering at the University of Kentucky

By

Adam Joseph Levy

Lexington, Kentucky

Director: Dr. William Chad Wedding, Assistant Professor of Mining Engineering

Lexington, Kentucky

2017

ABSTRACT OF THESIS

COMPARISON OF PERFORMANCE OF VORTECONE INERTIAL DUST SEPARATOR TO FLOODED-BED DUST SCRUBBER

Increasing incidence of Black Lung disease in miners since the early 1990s has concerned law makers and the mining industry. New regulations promulgated by MSHA in 2014 lowered the permissible limit of dust exposure of underground workers. The hazards of respirable coal dust have been common knowledge throughout the mining industry since the enactment of the 1969 Federal Coal Mine Health and Safety Act, and many administrative controls have been put in place since its enactment.

The purpose of this thesis is to analyze the performance of a Vortecone scrubber, used in the automotive industry to remove paint overspray from the air, for removing coal dust with an emphasis on respirable coal dust. Comparisons are made to a very effective scrubbing technology already in use in many underground coal mines, a flooded-bed scrubber system. This system is typically mounted on a continuous miner, and used to scrub contaminated air of unwanted particulate matter. Per the results of this study, a Vortecone appears to remove a greater amount of respirable dust from an airstream than a flooded-bed scrubber, and carries with it several operational advantages which are discussed.

KEYWORDS: Respirable Dust, Black Lung, Vortecone, Health and Safety

Adam Joseph Levy

4/26/2017

COMPARISON OF PERFORMANCE OF VORTECONE INERTIAL DUST SEPARATOR TO FLOODED-BED DUST SCRUBBER

By

Adam Joseph Levy

Dr. William Chad Wedding
Director of Thesis

Dr. Zach Agioutantis
Director of Graduate Studies

4/26/2017

DEDICATION

I dedicate this thesis work to the continuing effort to end Black Lung, a preventable industrial disease.

ACKNOWLEDGEMENTS

I want to thank my wife, Nicole, for her unconditional love and support. I would also like to thank my parents, June and David, who continue to support me in everything I do.

I would also like to thank my advisor, Dr. William C. Wedding, for his leadership, guidance, and support in my pursuit of my graduate degree. My colleagues Mr. Ed Thompson, Dr. Josh Calnan, Mr. Sampurna Arya, and Mr. Ashish Kumar also deserve recognition for their support in the completion of this research. Additionally, I thank my committee members Dr. Thomas Novak and Dr. Joseph Sottile for their excellent suggestions and academic support.

TABLE OF CONTENTS

LIST OF TABLES

LIST OF FIGURES

Chapter One: Introduction

Per a study conducted by the National Institute for Occupational Safety and Health (NIOSH) the incidence rate of coal workers' pneumoconiosis (CWP), and other chronic diseases related to respirable coal mine dust exposure, has been on the rise since the early 1990s (NIOSH, 2008). Because of these findings, the Mine Safety and Health Administration (MSHA) has promulgated new regulations further reducing the allowable exposure miners may have to respirable dust (MSHA, 2014). These recent findings and regulations have initiated a renewed effort in improving the underground mine environment by reducing individual dust exposure.

Dust is an inescapable byproduct of coal mining, because any breaking or crushing of coal or rock will generate dust. A portion of generated dust is in the respirable range, having an aerodynamic diameter less than 10 microns, and poses a significant health risk to miners (WHO, 1999). Various methods of reducing or controlling dust emissions have been tested over the years, and some have proven to be very successful and are in wide use today. Some primary methods include dilution and displacement by ventilation, wetting and capture by water sprays, and collection and filtration by dust collector (Kissell, 2003).

A large share of the dust in an underground coal mine is generated at the working face, where the coal is broken and gathered for transport (NIOSH, 2008). Therefore, individuals employed close to the working face are at the highest risk of developing CWP and many dust control technologies are employed close to the active workings in a mine (Kissell, 2003; NIOSH, 2008). These dust control technologies can be stationary or machine-mounted depending on the application (Kissell, 2003). One that has proven

particularly effective is the machine-mounted, flooded-bed dust scrubber system (Campbell et al., 1983). The system employs, (1) a steel mesh screen flooded with water to trap dust in water droplets, (2) a demister to remove those droplets from the airstream, and (3) a fan to move the air (Campbell et al., 1983). The system is very effective, and can eliminate over 90% of the dust from coal mine air (Collinet et al., 1990).

The aim of this project is to introduce a new scrubbing system called the Vortecone, invented at the University of Kentucky and employed by Toyota Manufacturing, into the mining industry and to compare its performance with that of a flooded-bed screen and demister system. Vortecones currently employed by Toyota are used on its automotive painting line to separate paint overspray from the air (Salazar, 2012). The comparison will be made by testing a scale model of the Vortecone in a laboratory setting and comparing the results to those obtained from laboratory testing on a flooded-bed screen and demister system.

Chapter Two: Review of Literature

2.1 History of Black Lung and Dust Regulation

Black Lung, also known as CWP, has existed since humanity starting mining coal (Arnold, 2016). Some of the earliest recorded recognition of the lung problems that coal miners were having, and linking the illness to coal dust, comes from British doctors in the 1830s (McIvor and Johnston, 2007). And as knowledge continued to grow into the early 1900s about the hazards of coal dust, little was done in the way of legislation controlling levels of respirable coal dust (Arnold, 2016). "By the 1950s, scientists had shown with near certainty that CWP could be caused exclusively by excessive exposure to coal dust" (Arnold, 2016). A strike by the United Mine Workers of America (UMWA) in 1968 initiated the creation of the 1969 Federal Coal Mine Health and Safety Act (Coal Act) (Arnold, 2016).

The incidence rate of CWP had been in steady decline since 1970, after the enactment of the Coal Act limited workers' exposure to respirable coal dust (NIOSH, 2008; Public Law 91-193, 1969). The Coal Act based the dust limitations on data from British prospective studies on CWP (Merchant, Taylor, and Hodous, 1986). However, research conducted by NIOSH has shown a rise in the incidence rate of CWP starting in the early 1990s (NIOSH, 2008). Therefore, the U.S. Department of Labor through MSHA proposed a new dust rule, called the Final Rule, aimed at lowering miners' exposure to respirable coal mine dust even further (MSHA, 2014). The Final Rule, effective August 1, 2016, lowered the permissible respirable dust exposure limit from 2.0 mg/m^3 to 1.5 mg/m^3 in the underground workings and from 1.0 mg/m^3 to 0.5 mg/m^3 in the intake air of an underground working place (U.S. Department of Labor, 2014). The Final Rule goes on

to say that decreasing the amount of respirable coal dust a worker is exposed to is "…the most effective means of preventing diseases caused by excessive exposure to such dust." (U.S. Department of Labor, 2014).

2.2 Epidemiology of Coal Workers' Pneumoconiosis

The term "black lung" comes from the legal definition of many diseases that affect the lungs of individuals who have worked in a coal mine (Castranova and Vallyathan, 2000). Black lung includes CWP, bronchitis, emphysema, and silicosis which are diseases that are caused by the constituents of coal mine dust (Castranova and Vallyathan, 2000). The reason for lumping diseases under one umbrella is that it is difficult to distinguish among them without direct examination of the lungs which can only occur post-mortem (Castranova and Vallyathan, 2000). CWP is further divided into two separate diseases, simple CWP and complicated CWP depending on the characteristics and progression of the disease in the lung (Castranova and Vallyathan, 2000). CWP starts as the simple variety, and upon continued exposure the lungs continue to fill with coal dust and complex CWP develops (Castranova and Vallyathan, 2000). Simple and complex CWP are separated by the size and number of zones in a radiograph of a miner's lungs that have varying opacity compared to heathy lung tissue (Castranova and Vallyathan, 2000). The disease progresses because of several interactions between lung tissue and particles including physical and chemical mechanisms (Castranova and Vallyathan, 2000).

Silicosis, usually found in conjunction with other diseases in coal miners, is caused by crystalline silica being deposited in the lungs (Castranova and Vallyathan, 2000). Silica can be a constituent of coal mine dust, depending on the conditions of the mine, and may affect the maximum respirable dust exposure for a mine (Castranova and Vallyathan,

2000). Silicosis is encountered in several occupations, and silica dust is much more dangerous than coal dust because of its reactivity (Castranova and Vallyathan, 2000).

CWP, once progressed to the complex stage, can be called Progressive Massive Fibrosis (PMF) which includes decreased lung function due to disease caused by inhalation of damaging particles (Castranova and Vallyathan, 2000). PMF can progress independently of exposure, so it is important for individuals to participate in monitoring of their lung heath if they are in occupations which expose them to respirable dust (Castranova and Vallyathan, 2000). PMF is typically the last stage of the disease, which includes vascular degeneration and declining lung function (Castranova and Vallyathan, 2000).

2.3 Dust Characterization

Coal mine dust consists of over 50 different elements and their oxides and some can be cytotoxic and carcinogenic (NIOSH, 1995; Castranova and Vallyathan, 2000). It can also contain several minerals, whose content and concentration in the dust vary by coal seam (NIOSH, 1995). Coal miners working in anthracite coal have higher rates of CWP than other miners (Castranova and Vallyathan, 2000). This is thought to be due in part to the increased toxicity of anthracite coal compared to coals of lower ranks (Castranova and Vallyathan, 2000).

Dust is generally characterized by the size of its particles, which can be measured in several different ways. Typically, when dust is looked at from the perspective of occupational health, the aerodynamic diameter is of interest (WHO, 1999). The aerodynamic diameter of a particle is defined as a particle having identical terminal settling velocity in calm air to a spherical particle of density 1 g/cm^3 "… regardless of its

geometric size, shape, and true density" (WHO, 1999). The reason aerodynamic diameter is of interest from a health perspective is because deposition of particles in the lungs is dictated by the aerodynamic diameter of the particle (WHO, 1999). A particle with a smaller aerodynamic diameter will travel deeper into the lungs than a particle with a larger aerodynamic diameter (WHO, 1999).

Coal mine dust has a wide size distribution, and the airborne constituent typically consists of particles less than 100 microns in aerodynamic diameter that are carried by the ventilating air (NIOSH, 1995; WHO, 1999). Particles larger in size may become airborne, but do not remain there for an extended period (WHO, 1999). A study by NIOSH (2007) that sized dust from 47 different coal mines, showed coal mine dust having a median diameter around 150 microns, with as much as 40% of the material being under 200 mesh (74 microns) in some samples. A more recent study conducted specifically in the return of a continuous miner section showed a median diameter of 48 microns with 90% of the total being below 104 microns (Barone et al. 2016). The "(a)irborne respirable dust in underground coal mines has been estimated to consist of 40% to 95% coal…" (NIOSH, 1995). This varies by coal rank, seam thickness, and mining method (NIOSH, 1995).

2.4 Dust and the Respiratory Tract

Any particle small enough to become airborne may be inhaled into the nose or mouth depending on the respiration of an individual (WHO, 1999). Inhalation probability depends on several factors, particularly the particles aerodynamic diameter (WHO, 1999). Particles that become airborne are about 100 microns and below in aerodynamic diameter (WHO, 1999). Once a particle is inhaled, there are five mechanisms that control the deposition of particles in airways. They are sedimentation, inertial impaction,

diffusion, interception, and electrostatic deposition (WHO, 1999). The primary mechanisms in human airways are sedimentation and inertial impaction (WHO, 1999). Particles having an aerodynamic diameter greater than 10 microns are typically deposited in an individual's nose and throat, while particles less than 10 microns continue to the thoracic region (WHO, 1999). Particles ranging from 10 to 4 microns are generally deposited in the airways of the lung, and particles less than 4 microns reach the alveoli of the lung, where gas exchange occurs (WHO, 1999). Figure 2.1 depicts a general schematic of particle deposition in the airways.

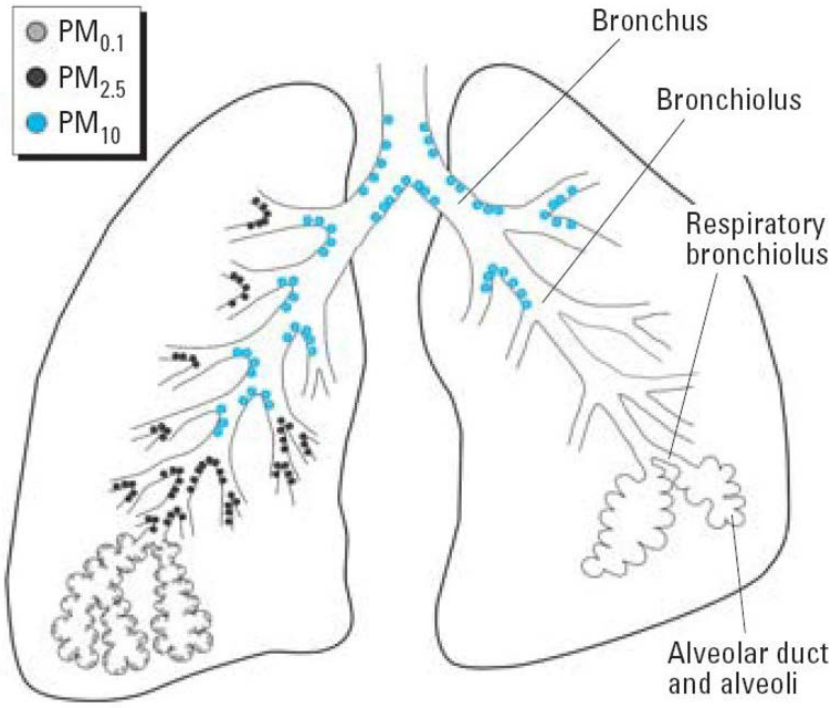

Figure 2.1: Depositional Regions of the Lung (NIOSH)

2.4 Overview of Particle Measurement Technology

Particulate matter is difficult to measure, because small particles represent relatively small masses and very sensitive instrumentation must be used (Amaral et al., 2015). Several methods for measuring particles exist today, with researchers needing to choose what type of measurement they wish to have, as well as the cost of the device (Amaral et al., 2015). The smaller the particle becomes, the more difficult and expensive it becomes to measure accurately (Amaral et al., 2015). The types of instruments that measure particles can be broken up into three different methods - gravimetric, optical, and microbalance methods (Amaral et al., 2015).

Gravimetric methods of measuring aerosol concentration represent sampling that directly collects a representative sample from an airstream, deposits it on a plate or filter, and then pre- and post-weights that filter for an averaged mass concentration (Amaral et al., 2015). This method is commonly used for personal sampling in environmental situations, where many standards are written in terms of a certain mass per unit volume of air that a worker may be exposed to (Amaral et al., 2015). These systems can be relatively inexpensive to operate, and require centralized pre- and post-weighing of filters for accurate measurements (Amaral et al., 2015). However, for gravimetric sampling of very small particles, very sensitive weighing equipment must be employed in a controlled environment to ensure accurate measurements (U.S. EPA 2016). For example, when measuring particulate matter present in ambient air below 2.5 microns, the U.S. Environmental Protection Agency requires that equipment be in an environment with temperature controlled to within two degrees centigrade, between thirty and forty percent relative humidity, and relatively vibration-free to avoid error in the measuring process

(U.S. EPA, 2016). These conditions typically require the construction of a unique room with specialized air handling equipment to accommodate the requirements (U.S. EPA, 2016).

The second, optical methods, represents a very broad range of particle measurement equipment that can rely on light scattering, light absorption, or light extinction (Amaral et al., 2015). These methods all use the properties of light and their interaction with particles to determine a particles size or concentration of particles, such as passing a particle neatly through a laser beam and measuring the response (Amaral et al., 2015). Light extinction can involve shining a light across a test duct and determining the amount of light attenuation for certain dust concentrations (Amaral et al., 2015). These techniques are advantageous because they do not require that the particles be collected on a surface, and are simply examined while still airborne (Glenn and Craft, 1986). However, the response of light to a particle may not always be uniform, and may be affected by the size as well as the color of the particle (Glenn and Craft, 1986). Therefore, the material being measured must have a carefully measured reflective and refractive index to properly correlate particle size with light response (Manickavasagam and Mengüç, 1993). For coal particles (of certain particle sizes ranges) the increase in light response is not linear with respect to particle size, making it difficult to distinguish between two particles (i.e. a 3 micron particle producing a response very similar to a 3.5 micron particle) (Manickavasagam and Mengüç, 1993). Therefore, without proper calibration, some optical machines may misrepresent the distribution of particle-size when measuring coal dust particles.

Finally, microbalance methods require very finely tuned micro scales to weigh individual particles or batches of particles to determine an exposure (Amaral et al., 2015). These instruments are typically expensive and involve a very small vibrating mass with a collection plate on top (Amaral et al., 2015). The vibrating mass will change frequency when particles are deposited on the collection plate; thus, a response can be measured and correlated with mass (Amaral et al., 2015). In this study, optical particle sizing methods are used for their quick readout time, one-step measurement (not requiring special sample handling and storage), and relatively low entry cost for the measuring devices.

2.5 Dust Controls in Underground Coal Mines

Dust is controlled in several ways including dilution and displacement by ventilation, wetting and capture by water sprays, and collection and filtration by dust collector (Kissell, 2003). These methods are aimed at reducing local dust concentration levels for the health and safety of the workers (Kissell, 2003). A large majority of dust in an underground coal mine is generated at the active working face, whether that be a continuous miner or longwall shearer (Kissell, 2003). Therefore, most dust control techniques are employed at or near the active workings of a mine (Kissell, 2003). Also, multiple dust control methods are typically employed at once because no single method, besides removing the worker from the dusty environment, eliminates exposure (Kissell, 2003).

Dilution by ventilating air serves to reduce the concentration of dust by supplying relatively fresh air to areas where workers are present (Kissell, 2003). This method can be useful if workers can be placed in the fresh air instead of standing in dirty or dusty air (Kissell, 2003). Displacement by ventilating air works in a similar fashion, but intends to

use the velocity of ventilating air to move the dust away from workers (Kissell, 2003). This method, noted by Kissell (2003), "… is the most effective dust control technique available…" but is difficult to implement. "The cost and technical barriers to increased airflow can be substantial…" and are not always fiscally or technically feasible (Kissell 2003).

Water sprays aim to accomplish two objectives, wetting newly broken material and capturing airborne particles inside water droplets (Kissell, 2003). Wetting of newly broken material is an extremely valuable tool in controlling dust, Kissell (2003) notes, with a large portion of dust remaining on the surface of the material. Wetting of the material effectively captures the dust and prevents it from becoming airborne (Kissell, 2003). Sprays may be located on the mining machines themselves, as well as on any coal/rock breaking equipment to limit dust generated from the additional crushing of material (Kissell, 2003).

Another goal of water sprays is to capture dust once it has become airborne by creating many fine water droplets (Kissell, 2003). This works well in theory as well as in the laboratory, but there are drawbacks to the system in practice in an underground coal mine. Kissell (2003) notes that water sprays only capture a small amount of airborne respirable dust in an underground coal mine, because not all the air passes directly by a water spray. Kissell (2003) goes on to say that the water sprays may also induce airflow that increases a worker's exposure to dust by displacing the dust away from the working face and towards the worker.

The final method that is primarily used in underground coal mines is collection and filtration (Kissell, 2003). These can range from cab filters on mobile equipment to

machine-mounted scrubbers that capture dust-laden air near the cutting drum on mining equipment and pass it through a flooded-bed screen and demister (Kissell, 2003). A machine-mounted scrubber's performance is a function of the capture and cleaning efficiencies of the device (Kissell, 2003). While the scrubber may perform under ideal conditions at a 90%-95% efficiency, if only 50% of the air is captured then the dust reduction will only be around 40-50% (Kissell, 2003). Also, these scrubbers are maintenance intensive with clogging screens reducing capture efficiency by reducing the airflow through the systems (Kissell, 2003). With the aim of this project being a technology transfer of a new scrubbing system to potentially replace a flooded-bed scrubber system, the next section will evaluate these systems in greater detail.

2.6 Flooded-Bed Scrubber Overview and Performance

The use of a flooded-bed scrubber mounted on a continuous miner was patented in 1983, and involved the use of a flooded-bed screen with sprayer, a demister, and a fan (Campbell et al., 1983). Dusty air drawn from near the cutting drum flows through a steel mesh screen, wetted by a water spray, where the dust particles are either captured on the screen itself, or inside the water droplets generated by air forcing water through the screen (Campbell et al., 1983). The air filled with water droplets passes through a mist eliminator which removes the water from the air by internal separation and gathers the dirty water in a sump for removal (Campbell et al., 1983). Finally, the air passes through an axial vane fan that serves at the primary air mover for the system (Campbell et al., 1983). Figure 2.2 depicts a system mounted on a continuous miner.

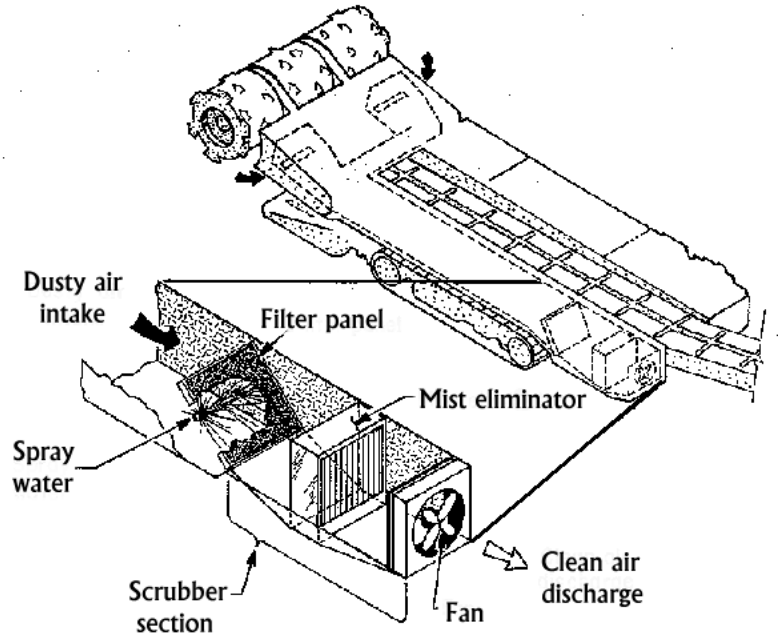

Figure 2.2: A Flooded-Bed Screen System on a Continuous Miner (NIOSH, 1997)

Studies have been conducted in laboratory settings as well as in the field on the performance of flooded-bed scrubber systems, with most testing being conducted by NIOSH (NIOSH, 2014; NIOSH, 1990). Laboratory testing conducted by NIOSH evaluated the capture performance of a flooded-bed scrubber and mist eliminator setup, with measurement upwind and downwind of the scrubber (NIOSH, 1990). These tests used a flooded-bed screen and demister identical to those used on a Joy 14CM, a commonly used continuous miner (NIOSH, 1990). A dust feeder introduced dust upwind of the system, which was then scrubbed, and the capture across the device was measured (NIOSH, 1990). Different screens were tested to determine the performance changes across screen by density and manufacturer (NIOSH, 1990). In testing, most filters could achieve a cleaning efficiency more than 90%, with slight variation attributed to manufacturer and screen density (NIOSH, 1990).

Field testing of machine-mounted flooded-bed scrubber systems included tests at three different mines that used such a machine-mounted system (NIOSH, 2014). The study looked at several different locations within each mine including machine operators as well as the return of the section for dust reduction when using the system (NIOSH, 2014). Per testing conducted by NIOSH (2014), reductions in dust levels in the return of each of the three mines were 91%, 85%, and 40% were achieved using the machine-mounted flooded-bed scrubber. This shows that this technology, in conjunction with machine-mounted sprays and other ventilation practices, serves to reduce the amount of dust present in the mine atmosphere (NIOSH, 2014).

2.7 Vortecone Scrubber Overview and Performance

The Vortecone is an inertial droplet separator invented at the University of Kentucky for use on an automotive paint line to capture paint overspray (Salazar, 2012). It accelerates contaminated air through the inlet portion of the device and then rapidly changes its direction, causing dust particles with high inertial energy to be transferred to the outer walls of the device (Salazar, 2012). Awaiting those particles is a sheet of water formed from the inlet of the device by water falling down all sides of the inlet and being accelerated along with the air (Salazar, 2012). The air then completes a turnaround 360° back to its original direction and exits the device (Salazar 2012). Figure 2.3 depicts a general schematic of the Vortecone, as depicted in the patent (Salazar, 2012). The inlet of the Vortecone is located at the top of the figure, with the air turning rapidly at the bottom and passing through one of two lobes that continue turning the air back to the original direction of travel to the outlet located near the bottom of the figure (Salazar, 2012).

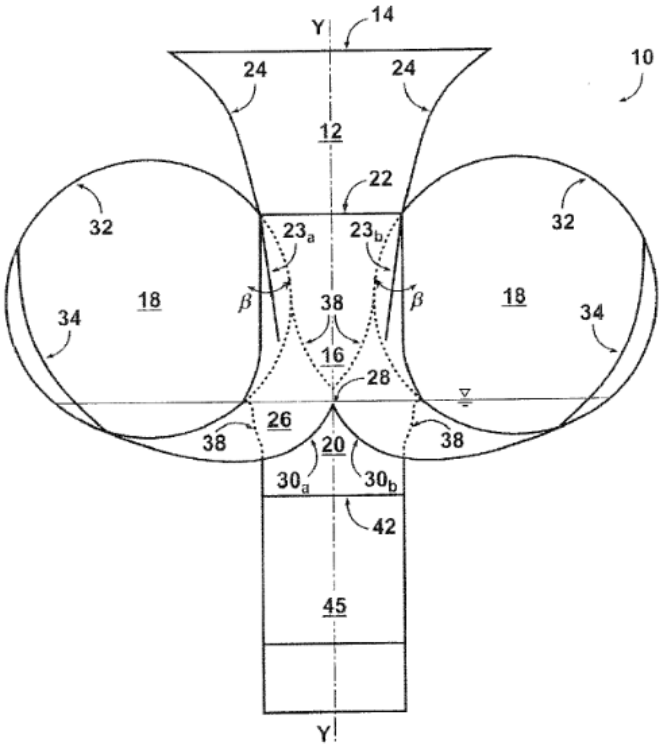

Figure 2.3: Schematic of a Vortecone Scrubber (Salazar, 2012)

A feasibility study was carried out by Tianxiang Li, Abraham J. Salazar, and Kozo Saito (2009) on using the Vortecone to remove fly ash from coal fired power plants. Small scale testing and numerical modeling of fly ash particles passing through a Vortecone were performed (Li et al., 2009). Their experimental results showed a cleaning efficiency of 99.8% for fly ash, with a 30% energy savings over a cyclone that is traditionally used for this task (Li et al., 2009). Fly ash and paint overspray both contain particles in the respirable range, and thus a transfer of the technology to cleaning coal mine dust was a logical next step for the technology.

Chapter Three: Testing Setup

3.1 Testing Setup Overview

A wind tunnel was constructed for testing both the Vortecone and flooded-bed scrubber in the Ventilation Laboratory at the University of Kentucky. Airflow through the tunnel is driven by a 25-horsepower centrifugal fan, model RBE-11, manufactured by Cincinnati Fan. This fan was selected based on desired flows and expected pressure drop through a 3:1 scale Vortecone, reduced from the geometry invented at the University of Kentucky, that was the target for testing. The fan was positioned at the entrance of the wind tunnel, serving as the start as well as the inlet of the wind tunnel. Figure 3.1 shows the Vortecone testing setup, with the fan inlet facing upward and outlet attached to the end of the aluminum duct pictured.

Figure 3.1: Vortecone Testing Setup

The duct is an 18” by 12” rectangular duct, constructed from aluminum sheet and an aluminum extrusion product. Each section of duct has an identical aluminum plate on each end for ease of assembly. This duct setup also makes the unit modular, so that some pieces of ductwork may be reused for both the Vortecone setup as well as the flooded-bed setup. Downwind of the fan is a Dwyer Instruments STRA Airflow Measurement Station (Dwyer Measurement Station), also having interior dimension of 18” by 12”. It uses a honeycomb structure to straighten the airflow, and then two pressure-averaging tubes are used to measure total and static pressure. The tubes are plumbed to the size of the station, so that measurements may be taken. Figure 3.2 shows the downwind side of the flow measurement station, with honeycomb flow straightener and pressure-averaging tubes. This device is calibrated by Dwyer, and has specified standards for distances from airflow disturbances such as fans and corners. Therefore, the geometry of the first portion of the wind tunnel, including the distance from the fan to the Dwyer Measurement Station (eight feet) and the distance from the measurement station to the first downward corner (three feet), is dictated by the product specifications.

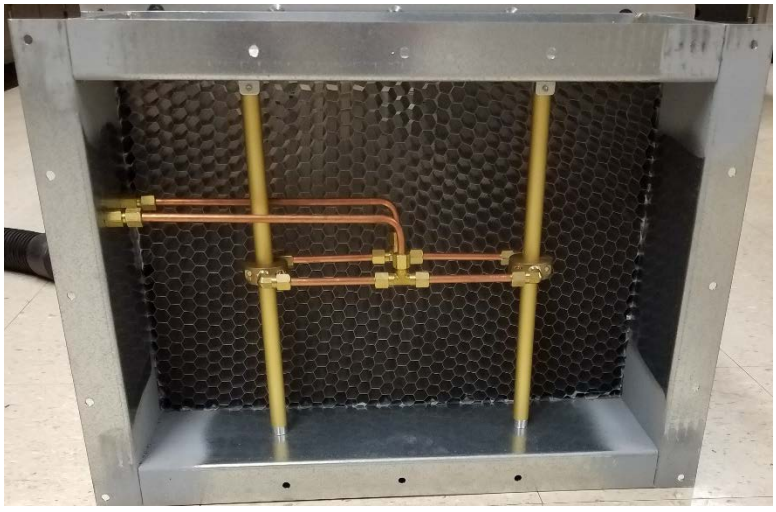

Figure 3.2: Inside of Dwyer STRA Airflow Measurement Station

In the case of the Vortecone setup, downwind of the Dwyer Measurement Station is a right-angle corner to direct flow downward and toward the Vortecone. The Vortecone was designed to be placed underneath an automotive painting line because of the required 100 linear feet per minute "…average air velocity over the open face of the booth (or booth cross section during spraying operations)…" (29 CFR § 1926.66(b)(5)(i), 1993). Therefore, Vortecones traditionally are situated with the inlet facing upward, and outlet facing downward underneath the entire cross-section of the painting line (Salazar 2012). Figure 3.3 depicts the portion of the test setup downwind of the Dwyer Measurement Station, with the Vortecone installed. To accommodate the traditional setup of the Vortecone, two corners are required to turn the flow downward into the Vortecone and then horizontal, so that the testing setup may reside inside the laboratory. Inside these corners are a generic HVAC turning vane and rail system provided by a local HVAC company. These turning vanes reduce the amount of shock loss through the corners, and are installed on both corners of the tunnel.

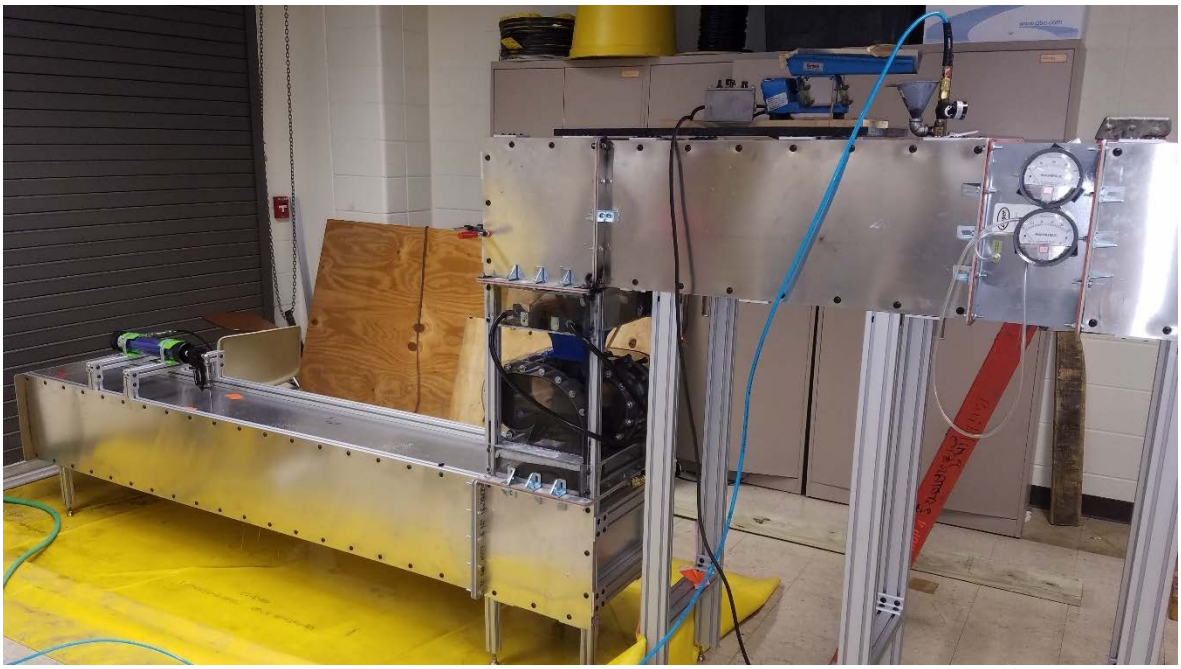

Figure 3.3: Vortecone Placement in Testing Setup

For the injection of dust into the system, a vibratory feeder meters the test dust into a conveying eductor, which sucks and aerosolizes in the material while conveying it into the duct. It is powered by a compressed air line that creates suction on the product inlet and accelerates the air through the discharge of the device into the test duct. Figure 3.4 shows a general cross section of an eductor, with more detail on the inner workings. Dust is ejected downward into the duct, but is rapidly accelerated in the direction of the airflow towards the Vortecone.

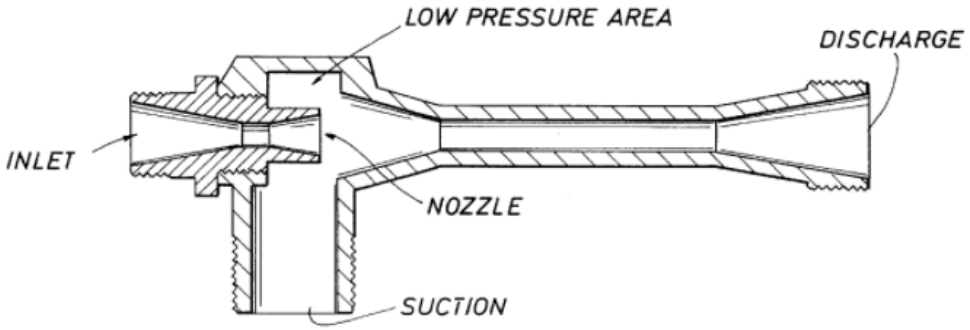

Figure 3.4: Conveying Eductor Layout (Crabtree, 1999)

The Vortecone is constructed from clear polycarbonate plates that are machined to fit 3D printed plastic parts that make up the inner geometry of the Vortecone. The 3D printed pieces are sandwiched between the polycarbonate sheets, and the whole assembly is bolted together. A 3D printed inlet is located at to the top of the device to aid in transition into the Vortecone and to reduce pressure loss. Figure 3.5 shows the test Vortecone in early stages of construction, with 3D printed parts sandwiched between clear polycarbonate sheets and held together with clamps. Once assembled, all seams were sealed with sealing compound.

Figure 3.5: Vortecone in Early Stages of Construction

After the air and dust exits the bottom outlet of the Vortecone through its two mirrored outlets, the flow is turned back horizontally and directed toward the sampling section, which will be explained in more detail in section 3.2. Figure 3.6 shows the underside of the Vortecone, with mirrored outlets at the bottom of the device. Figure 3.7 shows the Vortecone with blue inlet section installed as well as the orange water manifold, which

sheds a sheet of water around the periphery of the device to serve as the filter element inside the Vortecone as explained in Section 2.7. Water for the Vortecone is supplied by a traditional city water hose tap, flowing at approximately 10 gallons per minute. Figure 3.8 shows a top view of the Vortecone inlet and inside the water manifold.

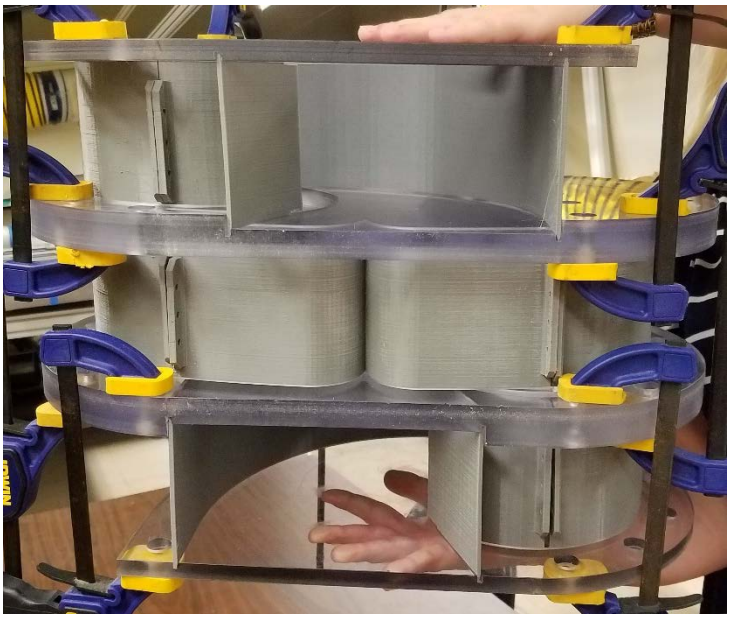

Figure 3.6: Bottom of the Vortecone

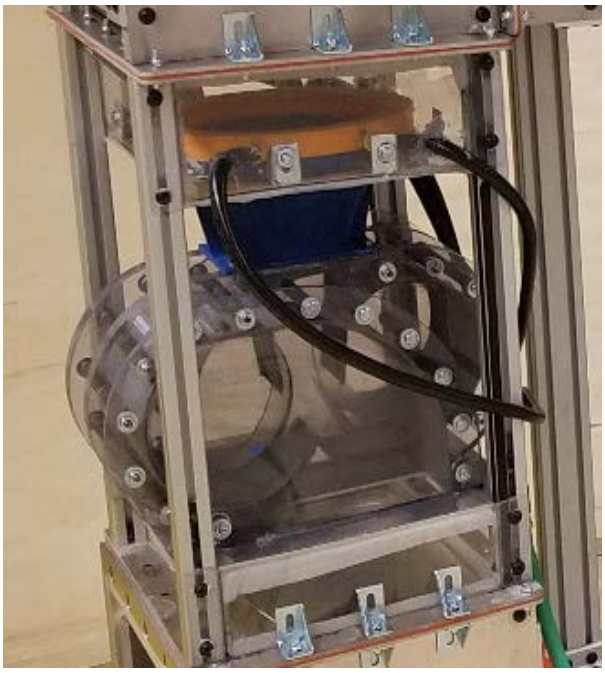

Figure 3.7: Vortecone with Inlet and Water Manifold Installed

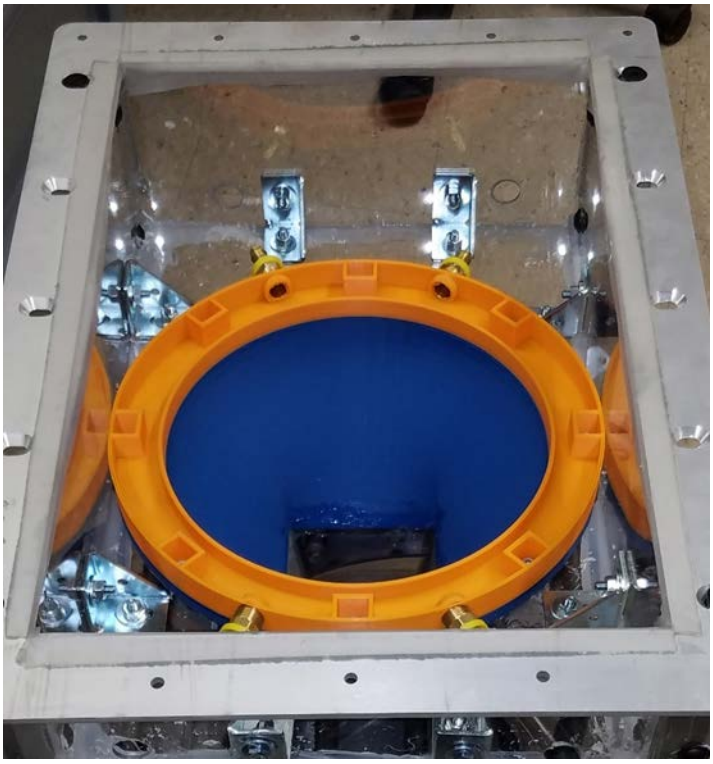

Figure 3.8: Top View of Water Manifold

A very similar setup is also used for the testing of the flooded-bed scrubber system with only minor changes. The fan, Dwyer Measurement Station, sampling section, and dust eductor are re-used from the Vortecone testing setup, simplifying construction. Figure 3.9 depicts the flooded-bed screen and demister testing setup. After the Dwyer Measurement Station a four-foot section of duct contains a 20-layer pleated flooded-bed screen. The screen is situated at approximately a 45-degree angle in the duct, as is seen in a traditional flooded-bed screen setup in the mining industry (Campbell et al., 1983). The demister section consists of sinusoidal demisting elements as employed by Joy Global, who supplied the demister fins as well as the flooded-bed screen. A single water spray supplies water to the screen as is typical for the setup, and is operated at approximately 10 gallons per minute from a traditional city water hose tap. Figure 3.10 shows the flooded-bed screen, demister, and water spray used for testing. The duct cross-section remains at 18” by 12”, and the flow travels straight through the entirety of the duct.

Figure 3.9: Flooded-Bed Scrubber Testing Setup

Figure 3.10: Flooded-Bed Screen and Demister Setup for Testing

Because testing of the flooded-bed scrubber required more time between control testing and filter testing, a more consistent auger feeder replaced the vibratory feeder. An auger feeder, a Techweigh Flex-Feed Volumetric Feeder 05 Series (Techweigh feeder), was chosen. The Techweigh feeder still feeds dust into the eductor in the same manner as the vibratory feeder. Figure 3.11 shows the Techweigh feeder setup, with internal hopper and feed screw leading to the end of the stainless-steel tube.

Figure 3.11: Techweigh Feeder Used for Flooded-Bed Setup

3.2 Sampling and Instrumentation

Isokinetic sampling of the airstream occurs approximately five feet from the start of the final duct section. In the case of the Vortecone setup this was five feet from the bottom corner, and in the case of the flooded-bed screen setup this was five feet from the rear of the demister. To properly sample in an isokinetic manner, the velocity of air entering the sampling probe must be identical to the velocity of the stream being sampled. This will prevent over or under sampling problems, which would misrepresent dust concentration in the airstream. Figure 3.12 depicts ideal isokinetic sampling, with streamlines undisturbed entering the sampling probe.

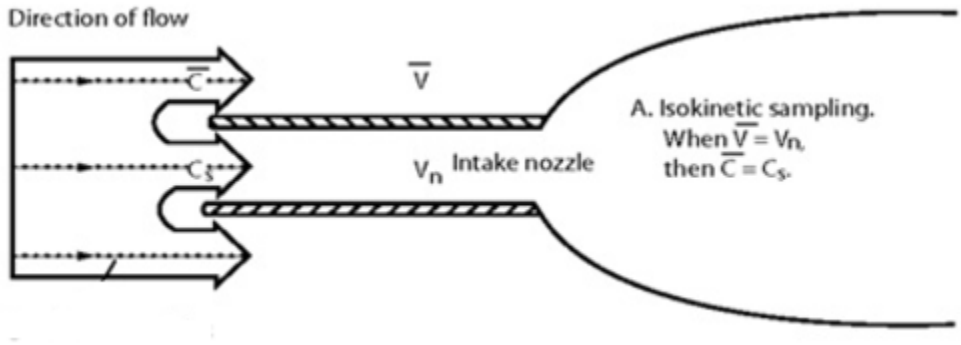

Figure 3.12: Isokinetic Sampling Visualization (Wilde, 2006)

To properly size the sampling probe for the testing setup, velocities for the ductwork had to be set. Velocities chosen for sampling were 535 fpm and 340 fpm, so an isokinetic sampling probe with interchangeable tips was constructed. The two tips were designed with a sample flow rate of 0.035 cubic feet per minute (1 liter per minute) sampling rate of the particle measuring device. To accommodate this flow rate, a simple calculation of dividing the flow by the velocity of the chosen test velocities gave the desired area, and therefore diameter hole, required for the probe tips to have an inlet velocity matching the

velocity of air in the tunnel. The probe tips were made to be 0.0318” and 0.0398” in diameter for the 535 fpm and 340 fpm flows respectively.

After being drawn through the isokinetic probe, the sampled air goes through the sampling train. The sampling train consists of a desiccant dryer, which is a tube within a large cylinder of desiccant that helps to eliminate any water droplets in the airstream as well as drying the aerosol sample as it passes through. After passing through the dryer, the sample goes through another isokinetic probe, which is located at a tee. This allows half of the flow to travel through the tee isokinetically (like a straw through the center of the tee) and the other half is forced to make the turn to the other leg of the tee. Figure 3.13 illustrates the entire sampling train.

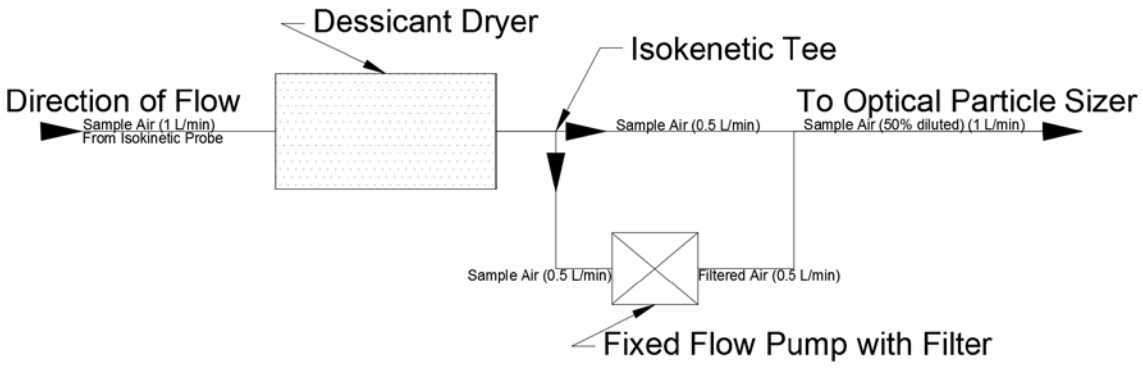

Figure 3.13: Sampling Train with Dilution Overview

Half the sample air, with flow rate cut in half (to 0.5 L/min) continues onward while the other half goes through a fixed flow pump with filter. This pump is set to 0.5 L/min (to ensure an even split of flows), and once filtered, rejoins the isokinetically split sample air to continue to the Optical Particle Sizer (OPS). The sampling train can also operate without any dilution, taking advantage of the isokinetic tee’s ability to split the flow in half without changing the sample, the sample flow rate can be increased to two liters per

minute at the isokinetic probe, and half of the sample can simply be sent through the fixed flow pump and into the atmosphere, allowing two additional sampling velocities, for a total of four, with only two isokinetic probe sizes. Figure 3.14 depicts the alternate way the sampling train may be set up.

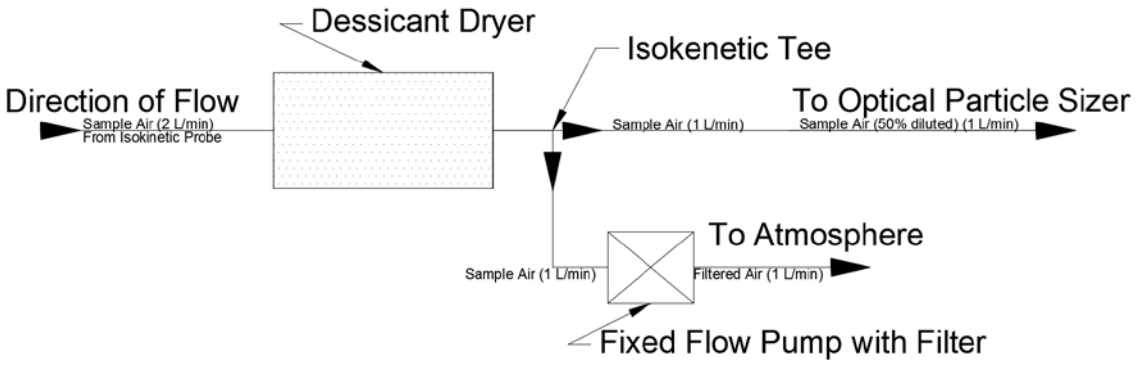

Figure 3.14: Sampling Train with No Dilution

The OPS, model OPS 3330, by TSI is the measurement device of choice for this study. It has a measurement range of carbon black particles from 0.357 micron to 14.59 micron. Figure 3.15 shows the OPS, with black inlet tip on the top of the instrument, and display panel for operation. Figure 3.16 depicts the inner workings of the OPS, showing the aerosol inlet, laser measurement and photodetection, and other operational parameters. The particle sizer reports particle counts in 17 size ranges, which are automatically chosen by the machine depending on the characteristics of the material being measured, as light response is not always linearly associated with particle size.

Figure 3.15: TSI Optical Particle Sizer (TSI)

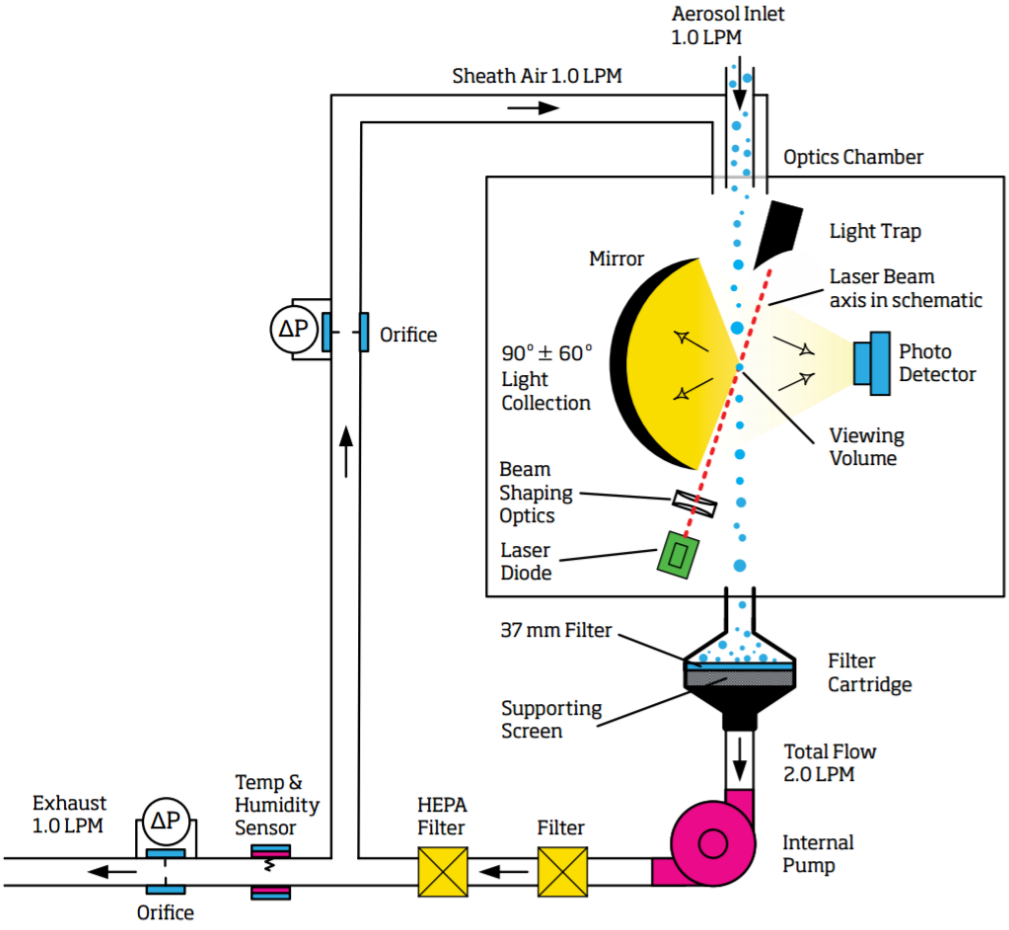

Figure 3.16: TSI OPS 3330 Internal Operation (TSI)

Chapter Four: Vortecone Testing

4.1 Testing Methodology

To begin testing, the fan was set using a variable frequency drive to provide the desired velocity through the tunnel and into the Vortecone. Then, a control test was performed by running only air and dust through the Vortecone, testing over 10 minutes and getting a total particle count for each of the 17 size bins from the OPS. After the control test was completed, another 10-minute test was conducted with air, dust, and water running through the Vortecone. With these two tests, a particle reduction could be calculated for each size bin on the OPS and a curve can be fitted to the data that approximates the capture rate of particles through the Vortecone. This reduction could then be compared to any size range of particles and give a theoretical capture of the device for the tested flow rate. For all testing in this report, a mineral black filler made from pulverized coal with 99.9% passing 325 mesh was used. The size distribution of this material, obtained from passing a representative sample through a Cilas 1064 Liquid Laser Particle Size Analyzer, is shown Figure 4.1. A full report of the size distribution measured by the Cilas machine can be found in Appendix A.

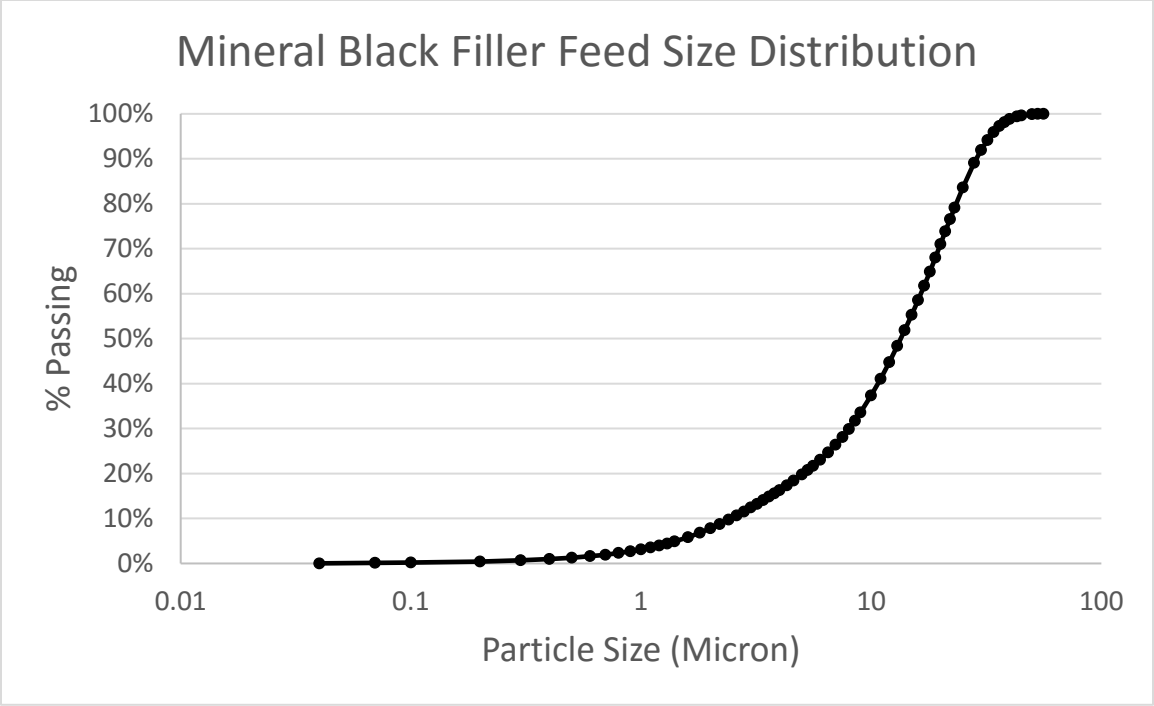

Figure 4.1: Feed Material Size Distribution

For the 535 fpm testing velocity, 10 replications were carried out with 10 minutes of control (dust and air) and 10 minutes of filter testing (dust, air, and water). The Appendix contains all the raw data for each test. For the 340 fpm testing velocity, only three replications were conducted because there were only small variations in results after more testing occurred at 535 fpm. Using this data, one can calculate theoretical capture and compare it to any theoretical coal dust distribution the Vortecone is required to filter.

4.2 System Curve Testing Results

A quantity and pressure survey was performed on the flooded-bed system with water running through the screen. Using the Dwyer Measurement Station to measure velocity pressure and total pressure while varying fan speed, a system curve can be developed and a power curve fit to the data. Figure 4.2 shows the results as well as a best-fit curve.

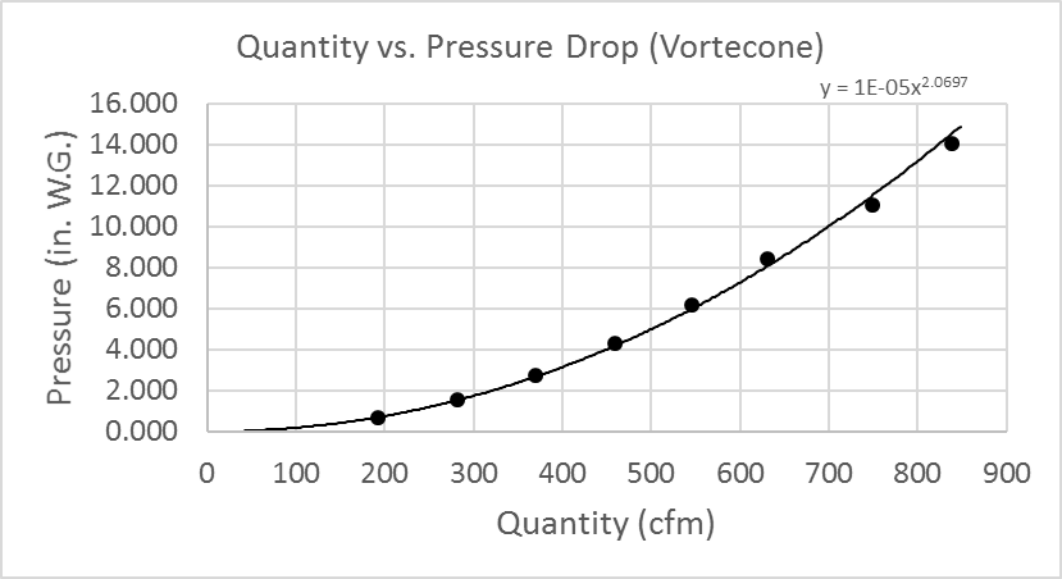

Figure 4.2: Vortecone System Curve

4.3 Dust Testing Results

Averaged over the 10 replications of testing that occurred, Table 4.1 shows the percent particle reduction for each of the size ranges provided by the OPS. There are some inconsistent results for measurements of particles below 1.488 micron, as some size ranges reported negative reduction in particle count with the Vortecone active. This is a product of coincidence error in the device. With too many small particles in the sample, the laser is overwhelmed and misreports particle counts in those size ranges. Therefore in the analysis of the data, any particle below 1.5 micron is considered not to be captured, because the OPS does provide useful information concerning the filters response to particles with respect to the Vortecone at the 50% dilution rate. As well, the 14.59+ size bin did not contain enough particles to be considered a representative sample in testing, so the results from that size bin will not be included in analysis. Figure 4.3 shows the curve of best fit generated for the 535 fpm test results. Only one of the two sampling

methods was used, which is the train with dilution, because flows beyond 535 fpm were difficult to achieve with the setup as constructed.

Table 4.1: Results for Vortecone Testing at 535 fpm

Particle Size Range (micrometer)	Average % Reduction
.357-.504	-22.2%
.504-.664	-20.4%
.664-.945	-1.7%
.945-1.114	6.1%
1.114-1.488	25.6%
1.488-1.999	48.0%
1.999-2.250	68.8%
2.250-2.545	77.3%
2.545-3.219	86.7%
3.219-4.170	90.9%
4.170-5.208	95.4%
5.208-6.513	98.6%
6.513-7.969	99.0%
7.969-9.423	99.2%
9.423-11.47	98.9%
11.47-14.59	96.9%
14.59+	76.1%

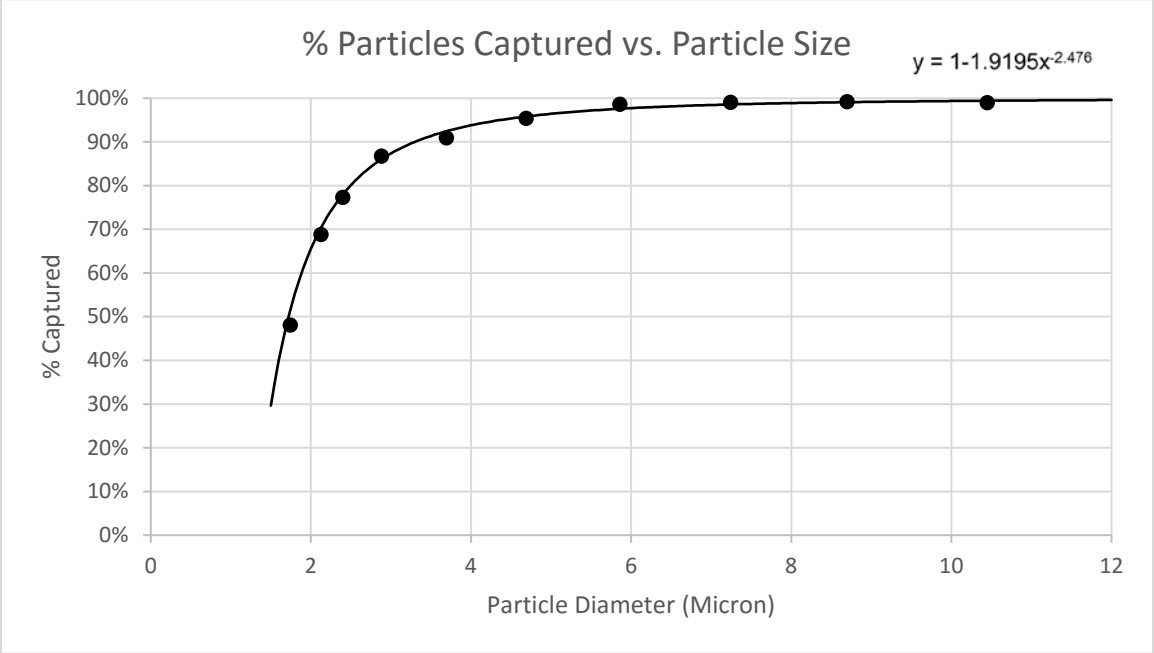

Figure 4.3: Vortecone Test Results Best Fit Curve at 535 fpm

Table 4.2 shows the averaged results for the three replications carried out at the 340 fpm test velocity, again with erroneous readings due to coincidence error in the particle size ranges below 1.5 micron. Also, very few particles were sampled above 14.59 micron so that data will not be used in analysis. Figure 4.4 shows the curve of best fit generated for the particle size ranges from 1.488 through 11.47 micron.

Table 4.2: Results for Vortecone Testing at 340 fpm

Particle Size Range (micrometer)	Average % Reduction
.357-.504	-25.5%
.504-.664	-22.5%
.664-.945	-20.4%
.945-1.114	-14.9%
1.114-1.488	-5.6%
1.488-1.999	2.5%
1.999-2.250	24.3%
2.250-2.545	39.9%
2.545-3.219	59.5%
3.219-4.170	79.2%
4.170-5.208	89.6%
5.208-6.513	94.2%
6.513-7.969	96.4%
7.969-9.423	97.7%
9.423-11.47	97.9%
11.47-14.59	94.8%
14.59+	61.6%

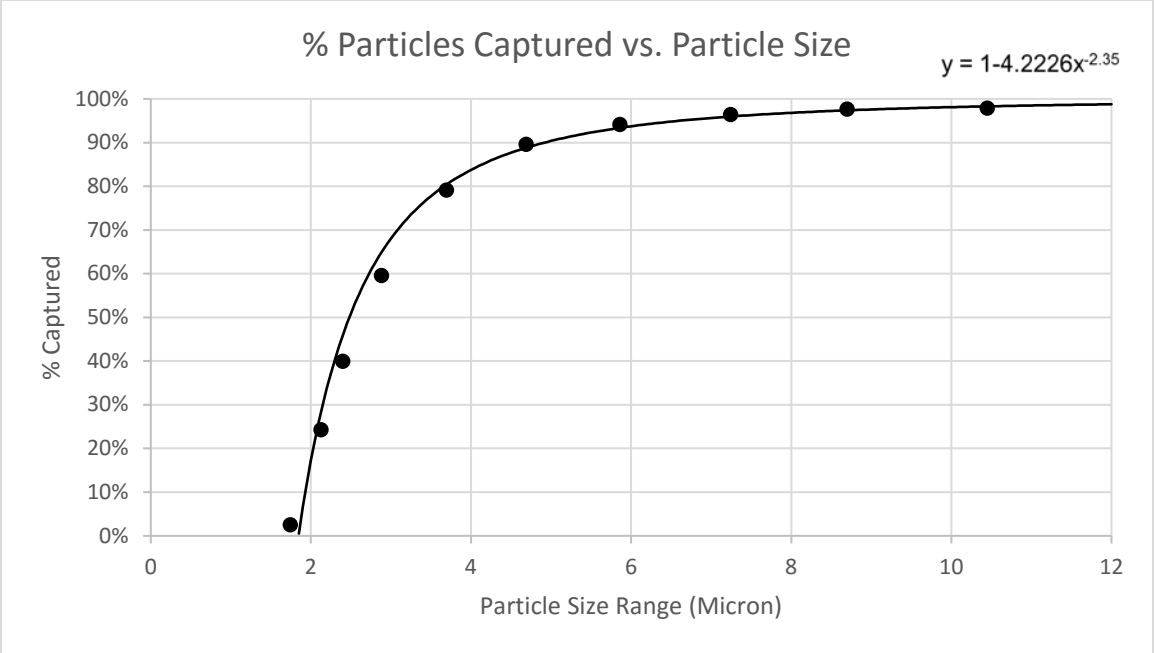

Figure 4.4: Vortecone Test Results Best Fit Curve at 340 fpm

Chapter Five: Flooded-Bed Screen Testing

5.1 Testing Methodology

For the flooded-bed screen and demister setup, control tests were performed on the ductwork with the screen and demister removed. Five samples of 10 minutes in duration each were taken at four velocities tested with the flooded-bed screen and demister. Both diluted and non-diluted sampling methods could be carried out, with dilution being used at the 340 fpm and 535 fpm speeds, and no dilution being used at the 680 fpm and 1070 fpm velocities.

After the control tests were carried out, the flooded-bed screen and demister were re-introduced to the setup, and testing occurred with the screen and demister in place and the sprayer flooding the screen with water to analyze its performance. Repeating each test five times in 10 minute durations at each of the four velocities. The results of are shown in Section 5.3. Each control test was compared to a filtered test to calculate a particle reduction with the flooded-bed screen and demister installed.

5.2 System Curve Testing Results

A quantity and pressure survey was carried out on the flooded-bed screen setup. This testing occurred with the water spray turned on. Using the Dwyer Measurement Station to measure pressure and quantity while changing the fan speed, a curve can be developed for analysis. Figure 5.1 shows the results as well as the curve of best fit.

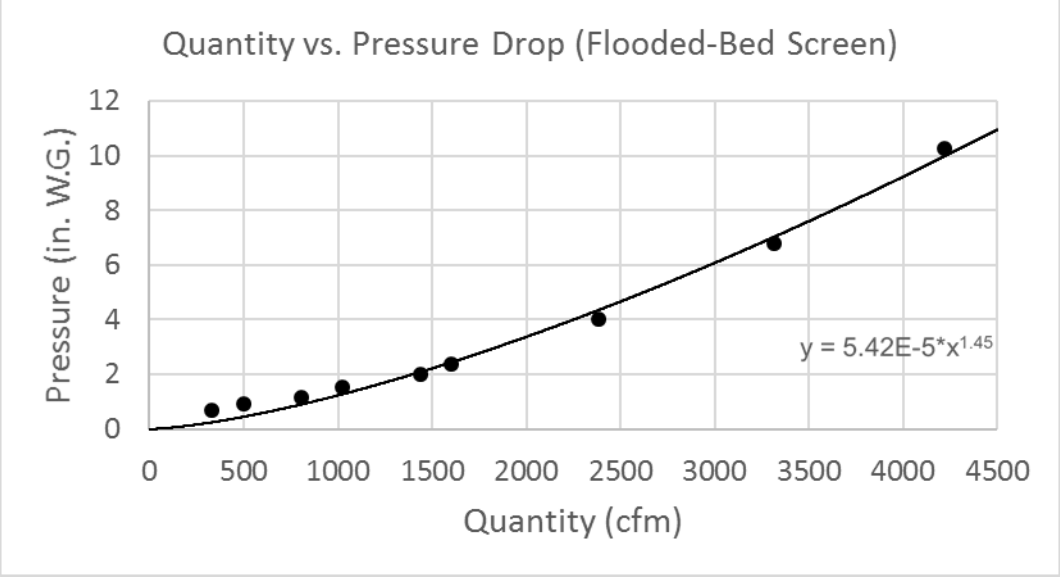

Figure 5.1: Flooded-Bed Screen System Curve

5.3 Dust Testing Results

In similar fashion to the Vortecone test results, some size fractions give inconsistent results because of coincidence error with the OPS. Therefore, any size fractions that report inconsistent particle numbers are not considered valid, and omitted from curve creation. Flooded-bed scrubbers typically do not operate at velocities as low as 340 fpm, and performance generally improves as velocity increases. At 340 fpm, the screen was not properly flooded with water and likely was not performing as intended. However, consistent results are found for particle size ranges above 1.488 micron. Another problem shared with the Vortecone, was that the 14.59+ micron size range did not contain enough particles to be considered valid and it was therefore omitted from curve fitting. The following tables and figures depict the results from each of the test velocities.

Table 5.1: Flooded-Bed Particle Reduction Results at 340 fpm

Particle Size Range (micrometer)	Average % Reduction
.357-.504	24.3%
.504-.664	24.7%
.664-.945	24.3%
.945-1.114	21.0%
1.114-1.488	37.4%
1.488-1.999	-19.2%
1.999-2.250	-20.8%
2.250-2.545	-18.0%
2.545-3.219	-5.3%
3.219-4.170	19.5%
4.170-5.208	48.1%
5.208-6.513	69.2%
6.513-7.969	82.4%
7.969-9.423	89.5%
9.423-11.47	92.8%
11.47-14.59	91.1%
14.59+	58.6%

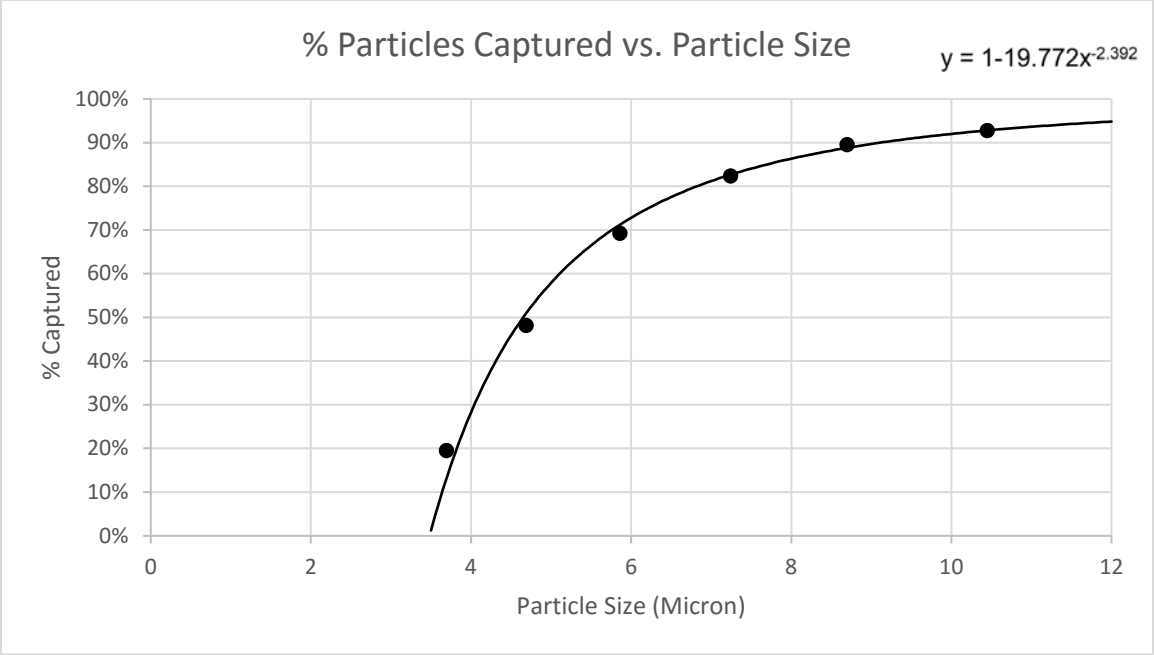

Figure 5.2: Flooded-Bed Particle Reduction Best Fit Curve at 340 fpm

Table 5.2: Flooded-Bed Particle Reduction Results at 535 fpm

Particle Size Range (micrometer)	Average % Reduction
.357-.504	-37.5%
.504-.664	-39.5%
.664-.945	-43.3%
.945-1.114	-37.6%
1.114-1.488	-51.4%
1.488-1.999	-2.0%
1.999-2.250	9.4%
2.250-2.545	21.2%
2.545-3.219	38.2%
3.219-4.170	58.4%
4.170-5.208	77.7%
5.208-6.513	87.9%
6.513-7.969	93.5%
7.969-9.423	96.3%
9.423-11.47	97.6%
11.47-14.59	96.6%
14.59+	86.2%

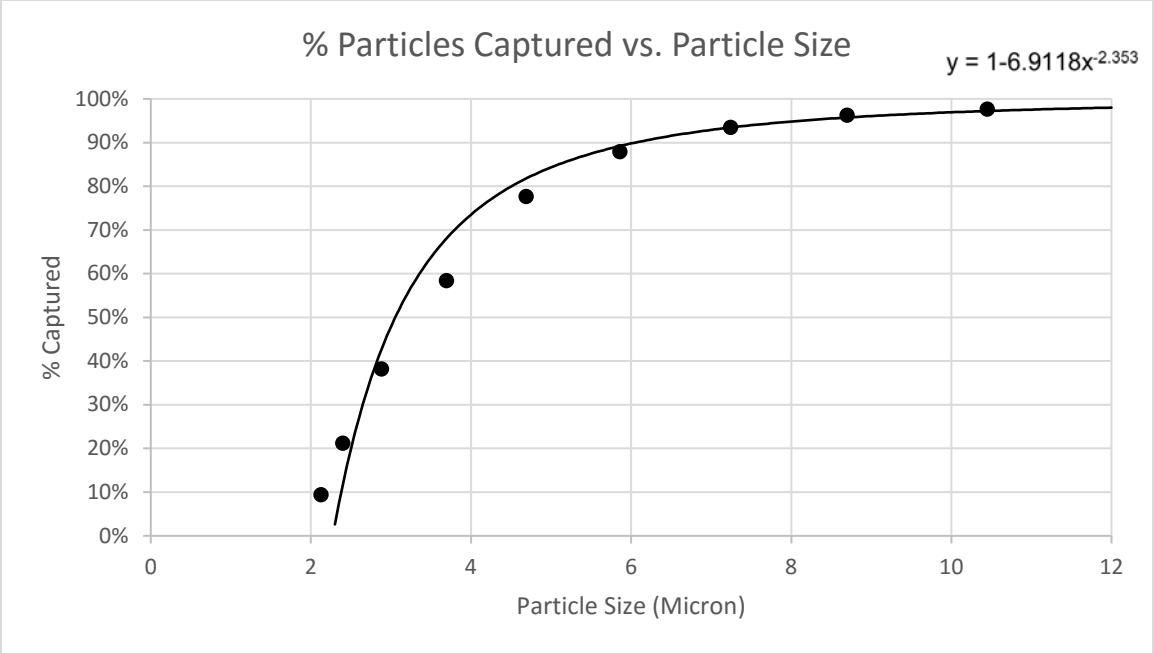

Figure 5.3: Flooded-Bed Particle Reduction Best Fit Curve at 535 fpm

Table 5.3: Flooded-Bed Particle Reduction Results at 680 fpm

Particle Size Range (micrometer)	Average % Reduction
.357-.504	-124.7%
.504-.664	-124.7%
.664-.945	-122.0%
.945-1.114	-118.6%
1.114-1.488	-237.2%
1.488-1.999	0.7%
1.999-2.250	27.3%
2.250-2.545	44.5%
2.545-3.219	63.4%
3.219-4.170	81.3%
4.170-5.208	91.2%
5.208-6.513	95.7%
6.513-7.969	97.9%
7.969-9.423	98.9%
9.423-11.47	99.2%
11.47-14.59	98.5%
14.59+	89.9%

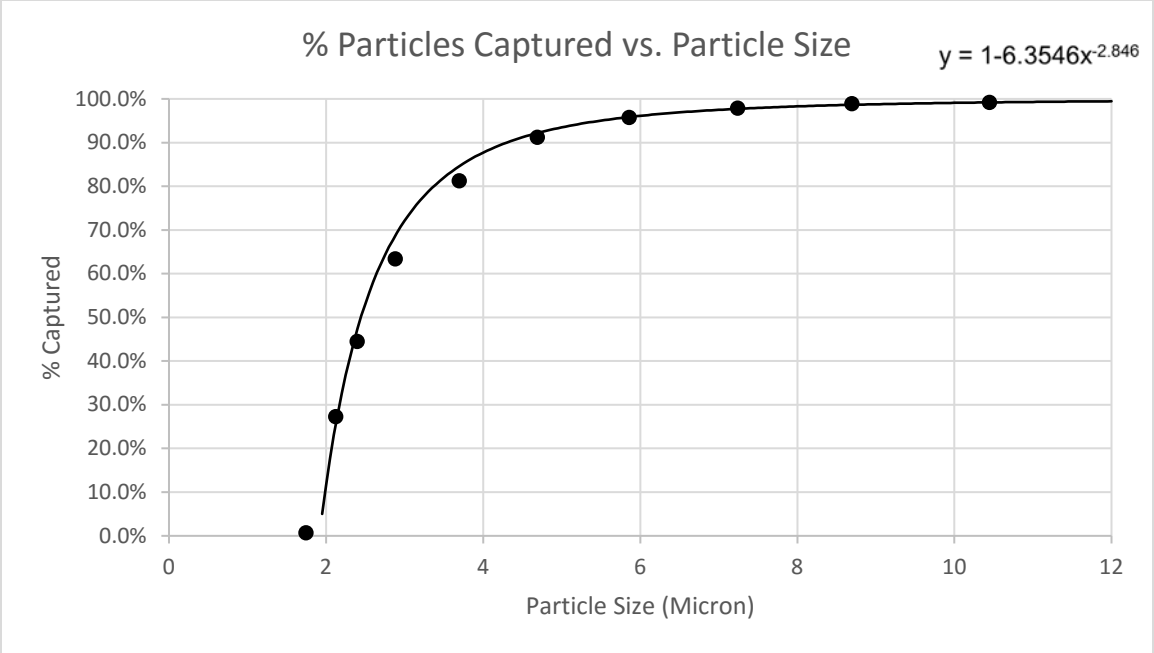

Figure 5.4: Flooded-Bed Particle Reduction Best Fit Curve at 680 fpm

Table 5.4: Flooded-Bed Particle Reduction Results at 1070 fpm

Particle Size Range (micrometer)	Average % Reduction
.357-.504	-7.9%
.504-.664	-9.3%
.664-.945	-14.0%
.945-1.114	-16.7%
1.114-1.488	-21.6%
1.488-1.999	-15.0%
1.999-2.250	-9.6%
2.250-2.545	0.3%
2.545-3.219	17.0%
3.219-4.170	41.6%
4.170-5.208	68.7%
5.208-6.513	83.6%
6.513-7.969	91.4%
7.969-9.423	95.3%
9.423-11.47	97.1%
11.47-14.59	96.2%
14.59+	83.1%

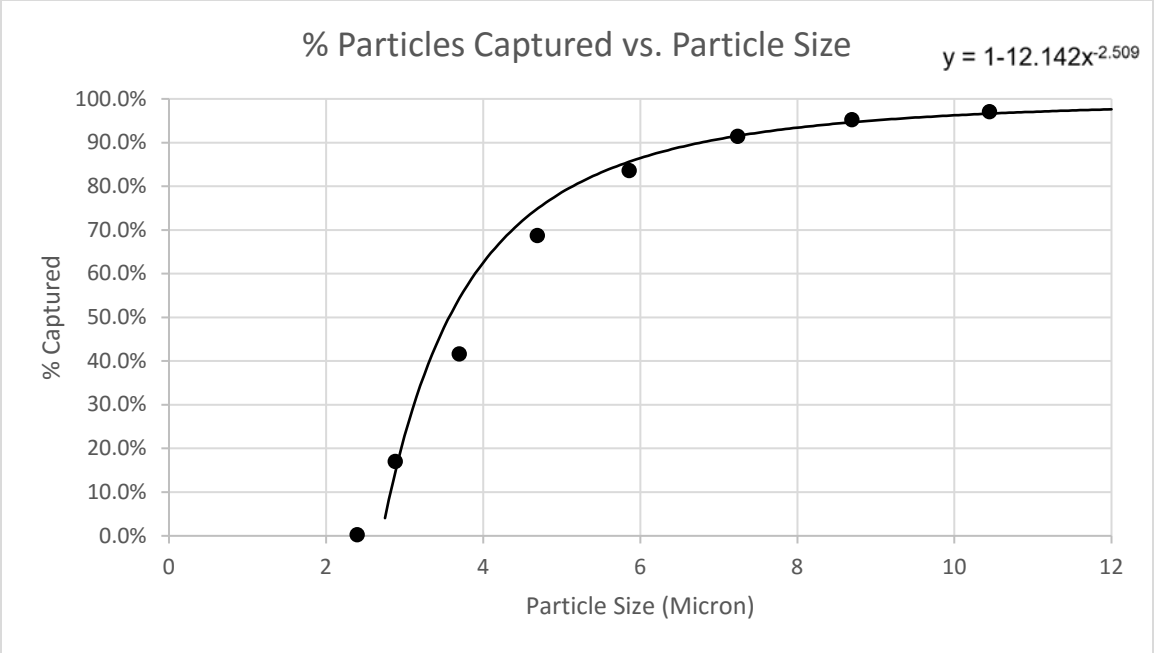

Figure 5.5: Flooded-Bed Particle Reduction Best Fit Curve at 1070 fpm

Chapter Six: Analysis & Discussion

For the Vortecone test setup, particle capture increases with increasing flow rate. This is to be expected, as the Vortecone uses a particles inertia to separate it from the airflow. Therefore, a higher flowrate through the Vortecone means particles will have a higher inertia, making them more likely to be captured on the opposite wall of the Vortecone. Also for the flooded-bed screen, there seems to be a general trend that with increasing velocity, there is an increase in particle capture. Further analysis of the data can be carried out by using the best fit curve generated from each individual trial, and calculating the mass and number of particles eliminated from the feed material. Using the curve of best fit from the Vortecone testing at 535 fpm, one can calculate a reduction in the particle count for any given size distribution by mass or count. Equation 1 below shows how volume percent reduction can be calculated for a given size fraction.

$$\%\, Remaining = Individual\, Volume\, \% * 1 - 1.9195(Individual\, Volume\, \%)^{-2.476} \quad (1)$$

After calculating the volume amount reduction, one can account for mass as well, by calculating the mass percentage for each individual size fraction represents, and applying the same technique. First, the average diameter of a particle for a given size range must be found, then the volume of that particle calculated. A necessary assumption that the particle is perfectly spherical needs to be made which, for smaller particles, can be a reasonable assumption. Once the average diameter is determined, the volume of a sphere of that diameter can be calculated, then multiplied by the density of the material. Equation 2 shows how the average mass of one particle from that size range may be calculated.

$$Avg.\, Particle\, Mass = \frac{4}{3} * \pi * \left(\frac{avg.diameter}{2}\right)^3 * density \quad (2)$$

Once a theoretical mass of one particle in a size range is found, multiplying that mass by the individual fraction percentage will give a relative mass contribution for each size fraction. This can then be used to compare mass reduction in each size fraction, and therefore in the feed. Equation 3 depicts how the mass contribution is calculated, and Equation 4 shows how the calculated theoretical mass reduction for a given size range is calculated.

$$Mass\ Contribution = Avg.Particle\ Mass * Individual\ \% \quad (3)$$

$$Mass\ Reduction = Mass\ Contribution * \%\ Remaining \quad (4)$$

This analysis was carried out for each test condition, for both the Vortecone and flooded-bed scrubber. Comparison was made with respect to the mineral black feed, 99.9% passing 325 mesh, using the entire size range of the feed as well as particles in the feed less than 10 microns. Table 6.1 shows the analysis as performed based on the best fit curve from each test condition, and compared to the entire feed distribution.

Table 6.1: Analysis of Particle Reduction from Feed for Each Test Condition

	From Entire Feed	
Test Conditions	Reduction by Count	Reduction by Mass
Vortecone 535 fpm	92.05%	99.92%
Flooded-Bed Scrubber 680 fpm	88.75%	99.90%
Vortecone 340 fpm	87.50%	99.74%
Flooded-Bed Scrubber 535 fpm	84.95%	99.59%
Flooded-Bed Scrubber 1070 fpm	82.94%	99.53%
Flooded-Bed Scrubber 340 fpm	78.05%	98.95%

Table 6.1 shows that both the flooded-bed scrubber and the Vortecone are very effective scrubbing technologies, removing over 98% of the mass from the mineral black feed in each test condition. However, their performance begins to differ when only looking at those particles most associated with health hazards to mine workers, particles below 10

microns, as can be seen in Table 6.2. The Vortecone, at 535 fpm, reduces the mass and count of particles below 10 microns at the highest rate, followed by the flooded-bed scrubber at 680 fpm. There appears to be a drop off for the flooded-bed scrubber as velocity increases, possibly because smaller particles start to pass through the screen more readily. The exact cause of this phenomenon is not known, but can be speculated with water more quickly clearing the flooded-bed screen, particles are free to pass through the mesh without contacting a water droplet.

Table 6.2: Testing Results Analyzed for Particles Under 10 Microns

	From <10 microns Particles	
Test Conditions	Reduction by Count	Reduction by Mass
Vortecone 535 fpm	78.99%	98.47%
Flooded-Bed Scrubber 680 fpm	70.20%	97.38%
Vortecone 340 fpm	67.39%	95.88%
Flooded-Bed Scrubber 535 fpm	61.09%	93.43%
Flooded-Bed Scrubber 1070 fpm	55.93%	91.52%
Flooded-Bed Scrubber 340 fpm	44.83%	83.74%

However, the impact of even smaller particles cannot be discounted whenever it comes to the occurrence of Black Lung. Therefore, analysis of particle capture less than 5 microns from the feed size distribution must also be considered. Table 6.3 shows how the devices performed, and that the Vortecone at 535 fpm significantly outperforms the flooded-bed scrubber at any velocity. With less maintenance than a flooded-bed screen system (no regular filter changes) and excellent performance, the Vortecone should make a significant and consistent reduction to respirable coal dust particles present in mine air.

Table 6.3: Testing Results Analyzed for Particles Under 5 Microns

Test Conditions	From <5 micron Particles	
	Reduction by Count	Reduction by Mass
Vortecone 535 fpm	61.50%	91.22%
Flooded-Bed Scrubber 680 fpm	45.65%	82.37%
Vortecone 340 fpm	41.81%	78.78%
Flooded-Bed Scrubber 535 fpm	32.07%	67.61%
Flooded-Bed Scrubber 1070 fpm	23.99%	57.03%
Flooded-Bed Scrubber 340 fpm	10.67%	31.72%

Chapter Seven: Conclusion

Testing conducted on a flooded-bed scrubber and Vortecone scrubber shows that both technologies are very effective at removing airborne particles, including those in the respirable range. Cleaning efficiencies exceeding 99% by mass were observed with both scrubbing technologies when compared to the entire feed distribution. However, looking at the performance in reduction in the number of particles under 10 microns, the Vortecone has an 8% reduction advantage by count. An even greater performance advantage is observed in the less than 5 micron particle size fraction with the Vortecone outperforming the flooded-bed system by nearly 16% by count. In addition, the greater reduction of the number of very small (less than 5 micron) particles from the airstream can also represent a significant health victory when it comes to respiratory disease in underground coal miners. With current MSHA regulations focusing on the mass of particles less than 10 microns current scrubbing technologies may look attractive, but without significant reduction in very small particles respiratory disease may still plague coal workers.

However, the increased performance does not come without an operational compromise in the form of increased air-power requirements. The Vortecone has significantly larger pressure drops than the flooded-bed screen system, which is caused in large part by the significant reduction of cross sectional area inside the inlet portion of the Vortecone required to accelerate incoming air into the device. For example, the air-power required to operate the Vortecone at the 535 fpm test condition is nearly eleven and a half times larger than the air-power required to operate the flooded-bed screen and demister setup at the same velocity. For the 340 fpm test condition, the air-power required to operate the

Vortecone is roughly eight and a half times larger than the flooded-bed screen system at the same velocity. Implementing Vortecone scrubbers in their current form would require more powerful, centrifugal fans be used to operate the device. These figures were calculated using the system curves developed in Section 4 and Section 5.

Another factor to consider is the maintenance of the scrubbing devices. The flooded-bed screen has a steel mesh that can become clogged and requires regular cleaning. The Vortecone does not have any such screen in place, and with clean water constantly flowing through the device, the filter media is always changing. This constant recirculation allows the Vortecone to maintain its efficiency for a much longer period, almost indefinitely, with proper operation. In terms of the machine-mounted flooded-bed scrubber system, whose performance is a function of capture and cleaning efficiency, if the screen were to never clog the capture efficiency would never decrease and the system could always operate optimally. A study by NIOSH in 2014 showed that in a single cut, the airflow through a flooded-bed scrubber reduced on average by 29%. The same study by NIOSH (2014) showed that a flooded-bed scrubber system, when working optimally, can reduce the amount of respirable dust by as much as 90%. Therefore, the Vortecone represents a significant improvement to the existing technology, by eliminating the reduction in capture efficiency created by factors such as poor maintenance, or loading of the flooded-bed screen during a cut. Replacing a flooded-bed screen and demister setup with a Vortecone scrubber would greatly increase the overall performance of a machine mounted scrubber system on a continuous miner, and ultimately reduce workers' exposure to respirable dust.

Chapter Eight: Future Work

With every experiment, new alterations to improve testing methodology and data analysis become apparent after experiments have concluded. For the experiments described herein the following changes are recommended. First, higher dilution ratios on the aerosol sampling system would allow the OPS to more accurately measure the particle size fractions that experienced high rates of coincidence in this testing. This would allow a finer definition of the lower tail of each distribution curve, which may become asymptotic with respect to capture, instead of a power degradation quickly to zero capture as shown in this study. Also, additional sampling velocities would allow a better understanding of the drop off in performance experienced on the flooded-bed screen system and allow one to find the optimum operation point for this setup. Additional isokinetic sampling with gravimetric samplers and multi-stage impactors would help to strengthen the analysis and provide a check against the performance of the OPS. Using multi-stage impactors that would give definite size fractions like the OPS would permit even finer comparison, particularly with the very fine size fractions (less than 5 micrometers).

Furthermore, the addition of a flow meter and pressure gauge on the water feed to both the Vortecone and flooded-bed screen sprayer would allow performance characteristics with respect to changes in water flow and pressure to be studied. Screens with more than twenty layers should also be compared to the Vortecone. Changes in the internal geometry of the Vortecone to reduce pressure loss should be considered, as well as changes to incorporate horizontal flow through the Vortecone.

Appendix

Table A.1: Test 1 Vortecone at 535 fpm

Particle Size Range (micrometer)	Dry Test Particle Count	Wet Test Particle Count	% Particle Reduction
.357-.504	3744530	1274648	66.0%
.504-.664	3875651	1311519	66.2%
.664-.945	5089582	548421	89.2%
.945-1.114	3326263	53958	98.4%
1.114-1.488	3234741	81405	97.5%
1.488-1.999	3600591	1397520	61.2%
1.999-2.250	1036994	262813	74.7%
2.250-2.545	818765	156467	80.9%
2.545-3.219	826154	94438	88.6%
3.219-4.170	348997	26888	92.3%
4.170-5.208	113804	4974	95.6%
5.208-6.513	43958	650	98.5%
6.513-7.969	15492	181	98.8%
7.969-9.423	4502	35	99.2%
9.423-11.47	1188	8	99.3%
11.47-14.59	206	6	97.1%
14.59+	37	8	78.4%

Table A.2: Test 2 Vortecone at 535 fpm

Particle Size Range (micrometer)	Dry Test Particle Count	Wet Test Particle Count	% Particle Reduction
.357-.504	3702730	4949333	-33.7%
.504-.664	3924602	5244129	-33.6%
.664-.945	5187017	5924601	-14.2%
.945-1.114	3347991	3362638	-0.4%
1.114-1.488	3112394	2460230	21.0%
1.488-1.999	3630406	2111893	41.8%
1.999-2.250	1039304	366652	64.7%
2.250-2.545	810609	204532	74.8%
2.545-3.219	808693	119308	85.2%
3.219-4.170	341048	28076	91.8%
4.170-5.208	111566	4661	95.8%
5.208-6.513	42981	698	98.4%
6.513-7.969	14863	154	99.0%
7.969-9.423	4352	35	99.2%
9.423-11.47	1196	7	99.4%
11.47-14.59	200	5	97.5%
14.59+	37	10	73.0%

Table A.3: Test 3 Vortecone at 535 fpm

Particle Size Range (micrometer)	Dry Test Particle Count	Wet Test Particle Count	% Particle Reduction
.357-.504	3770976	5180150	-37.4%
.504-.664	3849143	5079410	-32.0%
.664-.945	5103481	5987236	-17.3%
.945-1.114	3288075	3541629	-7.7%
1.114-1.488	3053992	2636745	13.7%
1.488-1.999	3420964	2015249	41.1%
1.999-2.250	955301	340449	64.4%
2.250-2.545	733158	189343	74.2%
2.545-3.219	728548	114194	84.3%
3.219-4.170	307077	29452	90.4%
4.170-5.208	102046	5088	95.0%
5.208-6.513	39194	577	98.5%
6.513-7.969	13795	133	99.0%
7.969-9.423	4235	50	98.8%
9.423-11.47	1101	17	98.5%
11.47-14.59	183	8	95.6%
14.59+	33	9	72.7%

Table A.4: Test 4 Vortecone at 535 fpm

Particle Size Range (micrometer)	Dry Test Particle Count	Wet Test Particle Count	% Particle Reduction
.357-.504	3932355	5058008	-28.6%
.504-.664	3718778	4821926	-29.7%
.664-.945	4799965	5355417	-11.6%
.945-1.114	3129331	3283816	-4.9%
1.114-1.488	2928940	2523165	13.9%
1.488-1.999	2840506	1600974	43.6%
1.999-2.250	757931	258987	65.8%
2.250-2.545	575365	144081	75.0%
2.545-3.219	564717	86162	84.7%
3.219-4.170	235934	25418	89.2%
4.170-5.208	78171	4308	94.5%
5.208-6.513	29635	535	98.2%
6.513-7.969	10801	128	98.8%
7.969-9.423	3274	19	99.4%
9.423-11.47	839	9	98.9%
11.47-14.59	179	1	99.4%
14.59+	57	3	94.7%

Table A.5: Test 5 Vortecone at 535 fpm

Particle Size Range (micrometer)	Dry Test Particle Count	Wet Test Particle Count	% Particle Reduction
.357-.504	3802163	4966351	-30.6%
.504-.664	3894735	5109510	-31.2%
.664-.945	4738247	5646052	-19.2%
.945-1.114	3108440	3463767	-11.4%
1.114-1.488	3017293	2683513	11.1%
1.488-1.999	2887901	1940708	32.8%
1.999-2.250	784582	338309	56.9%
2.250-2.545	600042	193609	67.7%
2.545-3.219	591285	111611	81.1%
3.219-4.170	243995	29610	87.9%
4.170-5.208	78611	4446	94.3%
5.208-6.513	29096	527	98.2%
6.513-7.969	9884	127	98.7%
7.969-9.423	2917	36	98.8%
9.423-11.47	753	10	98.7%
11.47-14.59	131	5	96.2%
14.59+	37	12	67.6%

Table A.6: Test 6 Vortecone at 535 fpm

Particle Size Range (micrometer)	Dry Test Particle Count	Wet Test Particle Count	% Particle Reduction
.357-.504	3774347	4812561	-27.5%
.504-.664	3704086	4663248	-25.9%
.664-.945	4669672	4896694	-4.9%
.945-1.114	3100765	3080064	0.7%
1.114-1.488	3079295	2397300	22.1%
1.488-1.999	3026099	1292864	57.3%
1.999-2.250	845161	198670	76.5%
2.250-2.545	660440	110472	83.3%
2.545-3.219	665992	64314	90.3%
3.219-4.170	278813	22081	92.1%
4.170-5.208	90527	3653	96.0%
5.208-6.513	33638	374	98.9%
6.513-7.969	11290	91	99.2%
7.969-9.423	3324	21	99.4%
9.423-11.47	924	11	98.8%
11.47-14.59	149	4	97.3%
14.59+	41	6	85.4%

Table A.7: Test 7 Vortecone at 535 fpm

Particle Size Range (micrometer)	Dry Test Particle Count	Wet Test Particle Count	% Particle Reduction
.357-.504	3849356	4957197	-28.8%
.504-.664	3625256	4783616	-32.0%
.664-.945	4558809	4971021	-9.0%
.945-1.114	3060752	3108092	-1.5%
1.114-1.488	2974110	2447541	17.7%
1.488-1.999	2677482	1311401	51.0%
1.999-2.250	727940	200784	72.4%
2.250-2.545	559027	112183	79.9%
2.545-3.219	564774	64967	88.5%
3.219-4.170	241532	22507	90.7%
4.170-5.208	80771	3958	95.1%
5.208-6.513	30021	380	98.7%
6.513-7.969	10215	98	99.0%
7.969-9.423	2900	30	99.0%
9.423-11.47	790	12	98.5%
11.47-14.59	153	14	90.8%
14.59+	31	12	61.3%

Table A.8: Test 8 Vortecone at 535 fpm

Particle Size Range (micrometer)	Dry Test Particle Count	Wet Test Particle Count	% Particle Reduction
.357-.504	3779116	5038021	-33.3%
.504-.664	3934301	4854698	-23.4%
.664-.945	4924740	5050861	-2.6%
.945-1.114	3232985	3146755	2.7%
1.114-1.488	3179482	2436596	23.4%
1.488-1.999	3235543	1314494	59.4%
1.999-2.250	894399	201600	77.5%
2.250-2.545	692493	111999	83.8%
2.545-3.219	697517	65262	90.6%
3.219-4.170	292246	21837	92.5%
4.170-5.208	96604	3609	96.3%
5.208-6.513	35704	356	99.0%
6.513-7.969	12380	86	99.3%
7.969-9.423	3576	13	99.6%
9.423-11.47	912	10	98.9%
11.47-14.59	140	2	98.6%
14.59+	47	6	87.2%

Table A.9: Test 9 Vortecone at 535 fpm

Particle Size Range (micrometer)	Dry Test Particle Count	Wet Test Particle Count	% Particle Reduction
.357-.504	3779116	5163623	-36.6%
.504-.664	3934301	5212568	-32.5%
.664-.945	4924740	5889103	-19.6%
.945-1.114	3232985	3627218	-12.2%
1.114-1.488	3179482	2745017	13.7%
1.488-1.999	3235543	1958649	39.5%
1.999-2.250	894399	331443	62.9%
2.250-2.545	692493	185021	73.3%
2.545-3.219	697517	105137	84.9%
3.219-4.170	292246	28653	90.2%
4.170-5.208	96604	4603	95.2%
5.208-6.513	35704	576	98.4%
6.513-7.969	12380	141	98.9%
7.969-9.423	3576	28	99.2%
9.423-11.47	912	7	99.2%
11.47-14.59	140	2	98.6%
14.59+	47	12	74.5%

Table A.10: Test 10 Vortecone at 535 fpm

Particle Size Range (micrometer)	Dry Test Particle Count	Wet Test Particle Count	% Particle Reduction
.357-.504	3812814	5023758	-31.8%
.504-.664	3795099	4915473	-29.5%
.664-.945	4965164	5370234	-8.2%
.945-1.114	3288336	3384038	-2.9%
1.114-1.488	3283756	2546627	22.4%
1.488-1.999	3388897	1607735	52.6%
1.999-2.250	962021	266355	72.3%
2.250-2.545	753746	151815	79.9%
2.545-3.219	762012	87566	88.5%
3.219-4.170	319905	25887	91.9%
4.170-5.208	104803	4038	96.1%
5.208-6.513	39225	456	98.8%
6.513-7.969	13702	94	99.3%
7.969-9.423	3928	25	99.4%
9.423-11.47	1041	10	99.0%
11.47-14.59	173	4	97.7%
14.59+	42	14	66.7%

Table A.11: Test 1 Vortecone at 340 fpm

Particle Size Range (micrometer)	Dry Test Particle Count	Wet Test Particle Count	% Particle Reduction
.357-.504	3103347	3886148	-25.2%
.504-.664	3861423	4670048	-20.9%
.664-.945	5018130	5808297	-15.7%
.945-1.114	3021606	3218677	-6.5%
1.114-1.488	2276729	2049050	10.0%
1.488-1.999	3771439	3102852	17.7%
1.999-2.250	1111352	668270	39.9%
2.250-2.545	862816	399676	53.7%
2.545-3.219	852733	261086	69.4%
3.219-4.170	373245	58255	84.4%
4.170-5.208	123701	9886	92.0%
5.208-6.513	47066	2131	95.5%
6.513-7.969	15762	446	97.2%
7.969-9.423	4610	82	98.2%
9.423-11.47	1134	21	98.1%
11.47-14.59	197	7	96.4%
14.59+	54	11	79.6%

Table A.12: Test 2 Vortecone at 340 fpm

Particle Size Range (micrometer)	Dry Test Particle Count	Wet Test Particle Count	% Particle Reduction
.357-.504	3052282	3802236	-24.6%
.504-.664	3772498	4602750	-22.0%
.664-.945	4792699	5819905	-21.4%
.945-1.114	2832742	3330238	-17.6%
1.114-1.488	2076705	2343663	-12.9%
1.488-1.999	3571370	3769543	-5.5%
1.999-2.250	1055295	893942	15.3%
2.250-2.545	826864	565767	31.6%
2.545-3.219	824221	385921	53.2%
3.219-4.170	359234	87704	75.6%
4.170-5.208	117245	14226	87.9%
5.208-6.513	43234	2932	93.2%
6.513-7.969	14377	601	95.8%
7.969-9.423	4062	102	97.5%
9.423-11.47	1047	27	97.4%
11.47-14.59	209	14	93.3%
14.59+	46	16	65.2%

Table A.13: Test 3 Vortecone at 340 fpm

Particle Size Range (micrometer)	Dry Test Particle Count	Wet Test Particle Count	% Particle Reduction
.357-.504	3004877	3811730	-26.9%
.504-.664	3709314	4616015	-24.4%
.664-.945	4729801	5861430	-23.9%
.945-1.114	2823743	3409483	-20.7%
1.114-1.488	2206353	2517291	-14.1%
1.488-1.999	3854590	4030010	-4.6%
1.999-2.250	1191267	979416	17.8%
2.250-2.545	960790	628855	34.5%
2.545-3.219	979170	429963	56.1%
3.219-4.170	434766	97862	77.5%
4.170-5.208	141272	15523	89.0%
5.208-6.513	51584	3190	93.8%
6.513-7.969	16794	631	96.2%
7.969-9.423	4805	131	97.3%
9.423-11.47	1195	24	98.0%
11.47-14.59	202	11	94.6%
14.59+	30	18	40.0%

Table A.14: Test 1 Flooded-Bed at 340 fpm

Particle Size Range (micrometer)	Control Test	Full-System Test	% Particle Reduction
.357-.504	2030615	1524135	24.9%
.504-.664	2285274	1701992	25.5%
.664-.945	2936138	2195286	25.2%
.945-1.114	1988004	1553249	21.9%
1.114-1.488	1869339	1155991	38.2%
1.488-1.999	5748640	6772015	-17.8%
1.999-2.250	2383376	2842883	-19.3%
2.250-2.545	2395837	2782025	-16.1%
2.545-3.219	3242555	3348109	-3.3%
3.219-4.170	2001435	1575758	21.3%
4.170-5.208	885200	447150	49.5%
5.208-6.513	419632	125695	70.0%
6.513-7.969	171329	29117	83.0%
7.969-9.423	53702	5440	89.9%
9.423-11.47	12050	812	93.3%
11.47-14.59	1235	110	91.1%
14.59+	73	50	31.5%

Table A.15: Test 2 Flooded-Bed at 340 fpm

Particle Size Range (micrometer)	Control Test	Full-System Test	% Particle Reduction
.357-.504	1974166	1595621	19.2%
.504-.664	2220169	1777184	20.0%
.664-.945	2856144	2291727	19.8%
.945-1.114	1936501	1625397	16.1%
1.114-1.488	1784442	1263056	29.2%
1.488-1.999	5748938	6763948	-17.7%
1.999-2.250	2390365	2809487	-17.5%
2.250-2.545	2408456	2730124	-13.4%
2.545-3.219	3255716	3257190	0.0%
3.219-4.170	2011141	1524265	24.2%
4.170-5.208	885711	432056	51.2%
5.208-6.513	417604	122081	70.8%
6.513-7.969	169201	28400	83.2%
7.969-9.423	52886	5412	89.8%
9.423-11.47	11733	808	93.1%
11.47-14.59	1258	95	92.4%
14.59+	101	33	67.3%

Table A.16: Test 3 Flooded-Bed at 340 fpm

Particle Size Range (micrometer)	Control Test	Full-System Test	% Particle Reduction
.357-.504	1977608	1505714	23.9%
.504-.664	2219191	1683163	24.2%
.664-.945	2848844	2177361	23.6%
.945-1.114	1928634	1541106	20.1%
1.114-1.488	1784217	1123342	37.0%
1.488-1.999	5723065	6841895	-19.5%
1.999-2.250	2377528	2881711	-21.2%
2.250-2.545	2389056	2828369	-18.4%
2.545-3.219	3228880	3407891	-5.5%
3.219-4.170	1992433	1606861	19.4%
4.170-5.208	874443	454113	48.1%
5.208-6.513	413533	127643	69.1%
6.513-7.969	167713	29927	82.2%
7.969-9.423	52660	5525	89.5%
9.423-11.47	11645	870	92.5%
11.47-14.59	1177	114	90.3%
14.59+	105	26	75.2%

Table A.17: Test 4 Flooded-Bed at 340 fpm

Particle Size Range (micrometer)	Control Test	Full-System Test	% Particle Reduction
.357-.504	1971727	1470084	25.4%
.504-.664	2215759	1643408	25.8%
.664-.945	2843726	2122826	25.4%
.945-1.114	1925443	1501473	22.0%
1.114-1.488	1759951	1060892	39.7%
1.488-1.999	5721976	6882455	-20.3%
1.999-2.250	2378395	2910207	-22.4%
2.250-2.545	2397288	2872223	-19.8%
2.545-3.219	3234886	3471791	-7.3%
3.219-4.170	1993687	1640642	17.7%
4.170-5.208	874567	462578	47.1%
5.208-6.513	412996	129142	68.7%
6.513-7.969	166892	29667	82.2%
7.969-9.423	52237	5515	89.4%
9.423-11.47	11435	842	92.6%
11.47-14.59	1229	116	90.6%
14.59+	93	51	45.2%

Table A.18: Test 5 Flooded-Bed at 340 fpm

Particle Size Range (micrometer)	Control Test	Full-System Test	% Particle Reduction
.357-.504	2024072	1458539	27.9%
.504-.664	2272396	1632391	28.2%
.664-.945	2918560	2107624	27.8%
.945-1.114	1970746	1483779	24.7%
1.114-1.488	1833192	1044537	43.0%
1.488-1.999	5697028	6875630	-20.7%
1.999-2.250	2354475	2912400	-23.7%
2.250-2.545	2359302	2883551	-22.2%
2.545-3.219	3174530	3495107	-10.1%
3.219-4.170	1951513	1660694	14.9%
4.170-5.208	853053	470423	44.9%
5.208-6.513	403830	131666	67.4%
6.513-7.969	163428	30486	81.3%
7.969-9.423	51460	5704	88.9%
9.423-11.47	11374	867	92.4%
11.47-14.59	1127	101	91.0%
14.59+	96	25	74.0%

Table A.19: Test 1 Flooded-Bed at 535 fpm

Particle Size Range (micrometer)	Control Test	Full-System Test	% Particle Reduction
.357-.504	1907345	2759881	-44.7%
.504-.664	2152112	3162821	-47.0%
.664-.945	2818376	4241403	-50.5%
.945-1.114	1974220	2835254	-43.6%
1.114-1.488	1826494	2901325	-58.8%
1.488-1.999	5964817	6000590	-0.6%
1.999-2.250	2503832	2192543	12.4%
2.250-2.545	2519629	1893856	24.8%
2.545-3.219	3402419	1962763	42.3%
3.219-4.170	2101040	794215	62.2%
4.170-5.208	921541	180590	80.4%
5.208-6.513	434781	43594	90.0%
6.513-7.969	176960	9234	94.8%
7.969-9.423	56081	1478	97.4%
9.423-11.47	13142	213	98.4%
11.47-14.59	1482	26	98.2%
14.59+	167	4	97.6%

Table A.20: Test 2 Flooded-Bed at 535 fpm

Particle Size Range (micrometer)	Control Test	Full-System Test	% Particle Reduction
.357-.504	2062915	2787486	-35.1%
.504-.664	2333558	3189128	-36.7%
.664-.945	3054307	4276582	-40.0%
.945-1.114	2117750	2847882	-34.5%
1.114-1.488	2052219	2943939	-43.5%
1.488-1.999	5903904	5972440	-1.2%
1.999-2.250	2427622	2194802	9.6%
2.250-2.545	2412155	1902072	21.1%
2.545-3.219	3215741	1996931	37.9%
3.219-4.170	1955981	822766	57.9%
4.170-5.208	854430	192067	77.5%
5.208-6.513	401246	48444	87.9%
6.513-7.969	163084	10304	93.7%
7.969-9.423	51864	1842	96.4%
9.423-11.47	12016	279	97.7%
11.47-14.59	1401	42	97.0%
14.59+	112	10	91.1%

Table A.21: Test 3 Flooded-Bed at 535 fpm

Particle Size Range (micrometer)	Control Test	Full-System Test	% Particle Reduction
.357-.504	2109915	2668098	-26.5%
.504-.664	2392556	3057900	-27.8%
.664-.945	3129815	4110635	-31.3%
.945-1.114	2160096	2747876	-27.2%
1.114-1.488	2101701	2826647	-34.5%
1.488-1.999	5883168	6100481	-3.7%
1.999-2.250	2403041	2274132	5.4%
2.250-2.545	2376296	1992196	16.2%
2.545-3.219	3138282	2126625	32.2%
3.219-4.170	1893690	898035	52.6%
4.170-5.208	821604	220602	73.1%
5.208-6.513	383787	60211	84.3%
6.513-7.969	154166	14411	90.7%
7.969-9.423	49221	2851	94.2%
9.423-11.47	11357	417	96.3%
11.47-14.59	1282	64	95.0%
14.59+	125	19	84.8%

Table A.22: Test 4 Flooded-Bed at 535 fpm

Particle Size Range (micrometer)	Control Test	Full-System Test	% Particle Reduction
.357-.504	1946506	2762734	-41.9%
.504-.664	2198229	3165848	-44.0%
.664-.945	2870130	4252844	-48.2%
.945-1.114	2002705	2840341	-41.8%
1.114-1.488	1840181	2949939	-60.3%
1.488-1.999	5940228	6017614	-1.3%
1.999-2.250	2480615	2211229	10.9%
2.250-2.545	2494455	1921929	23.0%
2.545-3.219	3365201	2020063	40.0%
3.219-4.170	2085344	834730	60.0%
4.170-5.208	924718	195998	78.8%
5.208-6.513	439038	49474	88.7%
6.513-7.969	179902	10650	94.1%
7.969-9.423	57652	1950	96.6%
9.423-11.47	13378	262	98.0%
11.47-14.59	1420	61	95.7%
14.59+	134	27	79.9%

Table A.23: Test 5 Flooded-Bed at 535 fpm

Particle Size Range (micrometer)	Control Test	Full-System Test	% Particle Reduction
.357-.504	1934065	2695705	-39.4%
.504-.664	2178232	3093029	-42.0%
.664-.945	2842269	4159946	-46.4%
.945-1.114	1982740	2791948	-40.8%
1.114-1.488	1803126	2880904	-59.8%
1.488-1.999	5901854	6091979	-3.2%
1.999-2.250	2473371	2257727	8.7%
2.250-2.545	2489778	1966848	21.0%
2.545-3.219	3370060	2071852	38.5%
3.219-4.170	2095819	854300	59.2%
4.170-5.208	928552	200553	78.4%
5.208-6.513	441662	50197	88.6%
6.513-7.969	181029	10724	94.1%
7.969-9.423	58295	1906	96.7%
9.423-11.47	13580	309	97.7%
11.47-14.59	1481	46	96.9%
14.59+	108	24	77.8%

Table A.24: Test 1 Flooded-Bed at 640 fpm

Particle Size Range (micrometer)	Control Test	Full-System Test	% Particle Reduction
.357-.504	1318760	3119999	-136.6%
.504-.664	1487414	3514044	-136.3%
.664-.945	1930163	4501920	-133.2%
.945-1.114	1231043	2888909	-134.7%
1.114-1.488	722210	2792089	-286.6%
1.488-1.999	5918342	5768626	2.5%
1.999-2.250	2680646	1888655	29.5%
2.250-2.545	2860854	1521518	46.8%
2.545-3.219	4090916	1420577	65.3%
3.219-4.170	2730164	482574	82.3%
4.170-5.208	1278761	106094	91.7%
5.208-6.513	648406	26403	95.9%
6.513-7.969	287999	5860	98.0%
7.969-9.423	100671	1147	98.9%
9.423-11.47	25762	197	99.2%
11.47-14.59	3193	52	98.4%
14.59+	198	6	97.0%

Table A.25: Test 2 Flooded-Bed at 640 fpm

Particle Size Range (micrometer)	Control Test	Full-System Test	% Particle Reduction
.357-.504	1357030	3059405	-125.4%
.504-.664	1526088	3445593	-125.8%
.664-.945	1979485	4417860	-123.2%
.945-1.114	1288293	2855526	-121.7%
1.114-1.488	811147	2771261	-241.6%
1.488-1.999	5871754	5874249	0.0%
1.999-2.250	2649514	1940254	26.8%
2.250-2.545	2818650	1575754	44.1%
2.545-3.219	4029825	1485715	63.1%
3.219-4.170	2693564	507283	81.2%
4.170-5.208	1270272	111773	91.2%
5.208-6.513	649185	27904	95.7%
6.513-7.969	291138	6156	97.9%
7.969-9.423	102675	1121	98.9%
9.423-11.47	26144	196	99.3%
11.47-14.59	3163	47	98.5%
14.59+	190	17	91.1%

Table A.26: Test 3 Flooded-Bed at 640 fpm

Particle Size Range (micrometer)	Control Test	Full-System Test	% Particle Reduction
.357-.504	1389413	3061815	-120.4%
.504-.664	1559662	3456485	-121.6%
.664-.945	2028229	4435764	-118.7%
.945-1.114	1342621	2873153	-114.0%
1.114-1.488	884519	2795290	-216.0%
1.488-1.999	5849190	5892189	-0.7%
1.999-2.250	2620291	1937876	26.0%
2.250-2.545	2783272	1570733	43.6%
2.545-3.219	3962871	1473688	62.8%
3.219-4.170	2646443	499403	81.1%
4.170-5.208	1252254	109625	91.2%
5.208-6.513	643928	27265	95.8%
6.513-7.969	288214	5970	97.9%
7.969-9.423	103349	1139	98.9%
9.423-11.47	26896	204	99.2%
11.47-14.59	3119	48	98.5%
14.59+	172	24	86.0%

Table A.27: Test 4 Flooded-Bed at 640 fpm

Particle Size Range (micrometer)	Control Test	Full-System Test	% Particle Reduction
.357-.504	1404827	3051270	-117.2%
.504-.664	1585031	3438180	-116.9%
.664-.945	2058750	4419204	-114.7%
.945-1.114	1380743	2863485	-107.4%
1.114-1.488	895038	2783020	-210.9%
1.488-1.999	5921076	5922193	0.0%
1.999-2.250	2640375	1950111	26.1%
2.250-2.545	2789699	1581618	43.3%
2.545-3.219	3935893	1482361	62.3%
3.219-4.170	2595546	500732	80.7%
4.170-5.208	1214908	109594	91.0%
5.208-6.513	617454	26915	95.6%
6.513-7.969	275309	5924	97.8%
7.969-9.423	97193	1084	98.9%
9.423-11.47	25152	222	99.1%
11.47-14.59	2977	37	98.8%
14.59+	180	23	87.2%

Table A.28: Test 5 Flooded-Bed at 640 fpm

Particle Size Range (micrometer)	Control Test	Full-System Test	% Particle Reduction
.357-.504	1385991	3104870	-124.0%
.504-.664	1563448	3488872	-123.2%
.664-.945	2030318	4469750	-120.2%
.945-1.114	1337563	2881075	-115.4%
1.114-1.488	843013	2787898	-230.7%
1.488-1.999	5928001	5822688	1.8%
1.999-2.250	2653163	1915863	27.8%
2.250-2.545	2810798	1552424	44.8%
2.545-3.219	3982275	1464483	63.2%
3.219-4.170	2633538	501719	80.9%
4.170-5.208	1235280	111209	91.0%
5.208-6.513	628996	27395	95.6%
6.513-7.969	280851	5984	97.9%
7.969-9.423	98538	1093	98.9%
9.423-11.47	25342	234	99.1%
11.47-14.59	3055	52	98.3%
14.59+	189	22	88.4%

Table A.29: Test 1 Flooded-Bed at 1070 fpm

Particle Size Range (micrometer)	Test 64 Trial 1	Test 68 Trial 1	% Particle Reduction
.357-.504	2385707	2759881	-15.7%
.504-.664	2686656	3162821	-17.7%
.664-.945	3455468	4241403	-22.7%
.945-1.114	2273360	2835254	-24.7%
1.114-1.488	2197251	2901325	-32.0%
1.488-1.999	5281591	6000590	-13.6%
1.999-2.250	2078650	2192543	-5.5%
2.250-2.545	2002038	1893856	5.4%
2.545-3.219	2546827	1962763	22.9%
3.219-4.170	1503917	794215	47.2%
4.170-5.208	661234	180590	72.7%
5.208-6.513	319946	43594	86.4%
6.513-7.969	135181	9234	93.2%
7.969-9.423	44591	1478	96.7%
9.423-11.47	10988	213	98.1%
11.47-14.59	1264	26	97.9%
14.59+	96	4	95.8%

Table A.30: Test 2 Flooded-Bed at 1070 fpm

Particle Size Range (micrometer)	Test 64 Trial 2	Test 68 Trial 2	% Particle Reduction
.357-.504	2533861	2787486	-10.0%
.504-.664	2869906	3189128	-11.1%
.664-.945	3700364	4276582	-15.6%
.945-1.114	2419744	2847882	-17.7%
1.114-1.488	2396120	2943939	-22.9%
1.488-1.999	5278409	5972440	-13.1%
1.999-2.250	2040817	2194802	-7.5%
2.250-2.545	1945200	1902072	2.2%
2.545-3.219	2448599	1996931	18.4%
3.219-4.170	1431820	822766	42.5%
4.170-5.208	626922	192067	69.4%
5.208-6.513	303978	48444	84.1%
6.513-7.969	127050	10304	91.9%
7.969-9.423	41154	1842	95.5%
9.423-11.47	9934	279	97.2%
11.47-14.59	1216	42	96.5%
14.59+	103	10	90.3%

Table A.31: Test 3 Flooded-Bed at 1070 fpm

Particle Size Range (micrometer)	Test 64 Trial 3	Test 68 Trial 3	% Particle Reduction
.357-.504	2602160	2668098	-2.5%
.504-.664	2947580	3057900	-3.7%
.664-.945	3791807	4110635	-8.4%
.945-1.114	2462408	2747876	-11.6%
1.114-1.488	2468081	2826647	-14.5%
1.488-1.999	5204673	6100481	-17.2%
1.999-2.250	2000492	2274132	-13.7%
2.250-2.545	1903405	1992196	-4.7%
2.545-3.219	2399279	2126625	11.4%
3.219-4.170	1404835	898035	36.1%
4.170-5.208	616316	220602	64.2%
5.208-6.513	299642	60211	79.9%
6.513-7.969	125997	14411	88.6%
7.969-9.423	41226	2851	93.1%
9.423-11.47	10058	417	95.9%
11.47-14.59	1205	64	94.7%
14.59+	109	19	82.6%

Table A.32: Test 4 Flooded-Bed at 1070 fpm

Particle Size Range (micrometer)	Test 64 Trial 4	Test 68 Trial 4	% Particle Reduction
.357-.504	2668759	2762734	-3.5%
.504-.664	3026314	3165848	-4.6%
.664-.945	3890923	4252844	-9.3%
.945-1.114	2512177	2840341	-13.1%
1.114-1.488	2530717	2949939	-16.6%
1.488-1.999	5123503	6017614	-17.5%
1.999-2.250	1960431	2211229	-12.8%
2.250-2.545	1863685	1921929	-3.1%
2.545-3.219	2354422	2020063	14.2%
3.219-4.170	1388820	834730	39.9%
4.170-5.208	616325	195998	68.2%
5.208-6.513	303487	49474	83.7%
6.513-7.969	129311	10650	91.8%
7.969-9.423	42569	1950	95.4%
9.423-11.47	10069	262	97.4%
11.47-14.59	1282	61	95.2%
14.59+	96	27	71.9%

Table A.33: Test 5 Flooded-Bed at 1070 fpm

Particle Size Range (micrometer)	Test 64 Trial 5	Test 68 Trial 5	% Particle Reduction
.357-.504	2500287	2695705	-7.8%
.504-.664	2834065	3093029	-9.1%
.664-.945	3650163	4159946	-14.0%
.945-1.114	2399748	2791948	-16.3%
1.114-1.488	2360842	2880904	-22.0%
1.488-1.999	5353834	6091979	-13.8%
1.999-2.250	2082172	2257727	-8.4%
2.250-2.545	1995701	1966848	1.4%
2.545-3.219	2530321	2071852	18.1%
3.219-4.170	1485237	854300	42.5%
4.170-5.208	651480	200553	69.2%
5.208-6.513	314350	50197	84.0%
6.513-7.969	131150	10724	91.8%
7.969-9.423	42817	1906	95.5%
9.423-11.47	10337	309	97.0%
11.47-14.59	1301	46	96.5%
14.59+	95	24	74.7%

CILAS
COMPAGNIE INDUSTRIELLE DES LASERS

PARTICLE SIZE DISTRIBUTION

CILAS 1064 Liquid

Range : 0.04 µm - 500.00 µm / 100 Classes

Sample ref.	: Sample_X_
Sample Name	:
Sample type	:
Comments	:
Liquid	:
Dispersing agent	:
Operator	:
Company	:
Location	:
Date : 06/07/2007	Time : 05:18:25AM
Index meas.	: 495
Database name	: Granulog

Ultrasounds	: 60	s
Obscuration	: 6 %	
Diameter at 10%	: 2.46	µm
Diameter at 50%	: 13.46	µm
Diameter at 90%	: 28.63	µm
Fraunhofer		
Density/Factor	----------	
Specific surface	----------	
Automatic dilution	: No / No	
Meas./Rins.	: 60s/60s/4	
SOP name	: Fraunhofer	

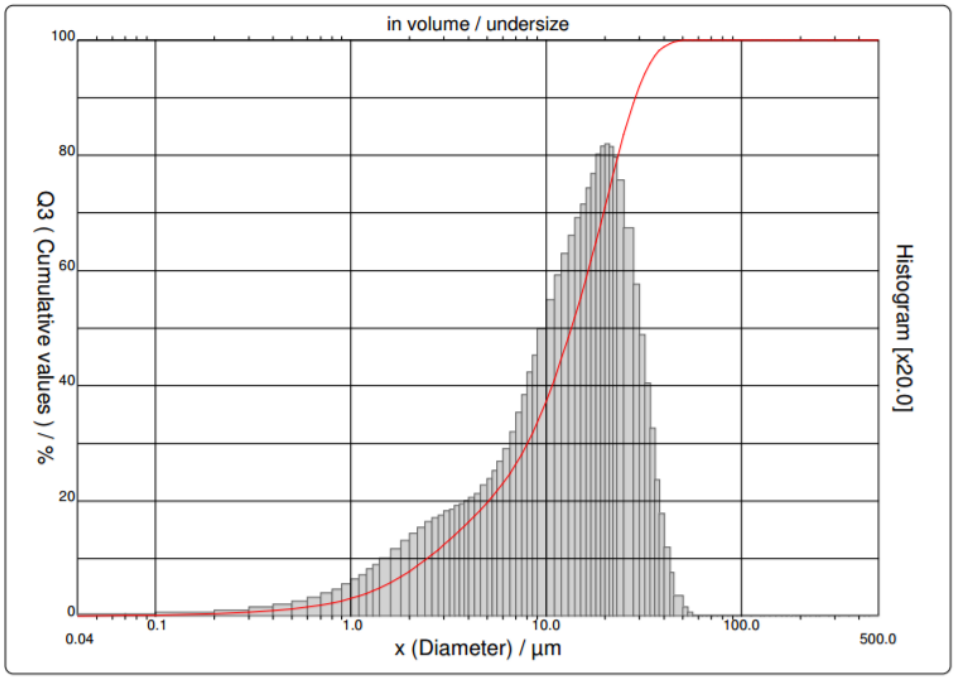

Serial nb : 1232 | Ref : 2.r176.m0.88A1818/6.00/495/m17.12.20.40.1Fh.20.20.40.Bh/Q-.0.0.0.0/600.0.15.g10.0.9.10.1.10.P6500.1.10.N.0/V 9.03/635

Figure A.1: Page 1 of Calis Report

PARTICLE SIZE DISTRIBUTION

CILAS 1064 Liquid

Range : 0.04 µm - 500.00 µm / 100 Classes

Sample ref.	: Sample_X_
Sample Name	:
Sample type	:
Comments	:
Liquid	:
Dispersing agent	:
Operator	:
Company	:
Location	:
Date : 06/07/2007	Time : 05:18:25AM
Index meas.	: 495
Database name	: Granulog

Ultrasounds	: 60	s
Obscuration	: 6 %	
Diameter at 10%	: 2.46	µm
Diameter at 50%	: 13.46	µm
Diameter at 90%	: 28.63	µm
Fraunhofer		
Density/Factor	----------	
Specific surface	----------	
Automatic dilution	: No / No	
Meas./Rins.	: 60s/60s/4	
SOP name	: Fraunhofer	

Standards classes in volume / undersize

x	0.04	0.07	0.10	0.20	0.30	0.40	0.50	0.60	0.70	0.80
Q3	0.02	0.10	0.17	0.41	0.68	0.97	1.28	1.60	1.94	2.31
q3	0.00	0.01	0.01	0.02	0.05	0.07	0.10	0.12	0.15	0.19
x	0.90	1.00	1.10	1.20	1.30	1.40	1.60	1.80	2.00	2.20
Q3	2.69	3.10	3.53	3.97	4.43	4.90	5.85	6.82	7.80	8.77
q3	0.23	0.27	0.31	0.35	0.40	0.44	0.50	0.57	0.65	0.71
x	2.40	2.60	2.80	3.00	3.20	3.40	3.60	3.80	4.00	4.30
Q3	9.72	10.65	11.55	12.41	13.25	14.05	14.83	15.58	16.31	17.37
q3	0.76	0.81	0.85	0.87	0.91	0.92	0.95	0.97	0.99	1.02
x	4.60	5.00	5.30	5.60	6.00	6.50	7.00	7.50	8.00	8.50
Q3	18.39	19.74	20.73	21.72	23.04	24.70	26.39	28.13	29.90	31.73
q3	1.06	1.13	1.19	1.25	1.34	1.45	1.59	1.76	1.91	2.11
x	9.00	10.00	11.00	12.00	13.00	14.00	15.00	16.00	17.00	18.00
Q3	33.58	37.33	41.07	44.75	48.35	51.85	55.26	58.56	61.78	64.92
q3	2.26	2.48	2.74	2.95	3.14	3.30	3.45	3.57	3.71	3.83
x	19.00	20.00	21.00	22.00	23.00	25.00	28.00	30.00	32.00	34.00
Q3	68.02	71.01	73.87	76.58	79.11	83.62	89.08	91.92	94.17	95.92
q3	4.00	4.07	4.09	4.07	3.97	3.77	3.36	2.87	2.43	2.01
x	36.00	38.00	40.00	43.00	45.00	50.00	53.00	56.00	60.00	63.00
Q3	97.25	98.16	98.81	99.42	99.66	99.92	99.98	100.00	100.00	100.00
q3	1.62	1.17	0.88	0.59	0.37	0.17	0.07	0.03	0.00	0.00
x	66.00	71.00	75.00	80.00	85.00	90.00	95.00	100.0	112.0	125.0
Q3	100.00	100.00	100.00	100.00	100.00	100.00	100.00	100.00	100.00	100.00
q3	0.00	0.00	0.00	0.00	0.00	0.00	0.00	0.00	0.00	0.00
x	130.0	140.0	150.0	160.0	170.0	180.0	190.0	200.0	212.0	224.0
Q3	100.00	100.00	100.00	100.00	100.00	100.00	100.00	100.00	100.00	100.00
q3	0.00	0.00	0.00	0.00	0.00	0.00	0.00	0.00	0.00	0.00
x	240.0	250.0	280.0	300.0	315.0	355.0	400.0	425.0	450.0	500.0
Q3	100.00	100.00	100.00	100.00	100.00	100.00	100.00	100.00	100.00	100.00
q3	0.00	0.00	0.00	0.00	0.00	0.00	0.00	0.00	0.00	0.00

x : diameter / µm Q3 : cumulative value / % q3 : density distribution

Serial nb : 1232 | Ref : 2.r176.m0.88A1818/6.00/495/m17.12.20.40.1Fh.20.20.40.Bh/Q-.0.0.0.0/600.0.15.g10.0.9.10.1.10.P6500.1.10.N.0/V 9.03/635

Figure A.2: Page 2 of Calis Report

References

29 CFR § 1926.66. 1993. “Criteria for design and construction of spray booths”. Occupational Health and Safety Administration.

Arnold, C. (2016). A scourge returns: Black lung in Appalachia. *Environmental Health Perspectives*. http://doi.org/10.1289/ehp.124-A13.

Amaral, S., de Carvalho, J., Costa, M., & Pinheiro, C. (2015). An Overview of Particulate Matter Measurement Instruments. *Atmosphere*, *6*(9), 1327–1345. http://doi.org/10.3390/atmos6091327.

Barone, T. L., Patts, J. R., Janisko, S. J., Colinet, J. F., Patts, L. D., Beck, T. W., & Mischler, S. E. (2016). Sampling and analysis method for measuring airborne coal dust mass in mixtures with limestone (rock) dust. *Journal of Occupational and Environmental Hygiene*, *13*(4), 284–292. https://doi.org/10.1080/15459624.2015.1116694.

Campbell, J. A. L., Moynihan, D. J., Roper, W. D., & Willis, E. C. (1983). DUST CONTROL SYSTEM AND METHOD OF OPERATION. United States: U.S. Patent Office.

Castranova, V., & Vallyathan, V. (2000). Silicosis and coal workers’ pneumoconiosis. *Environmental Health Perspectives*. http://doi.org/10.1016/B978-1-4557-0792-8.00051-9.

Colinet, J. F., Mcclelland, J. J., Erhard, L. A., & Jankowski, R. A. (1990). Laboratory Evaluation of Quartz Dust Capture of Irrigated-Filter Collection Systems for Continuous Miners. *Report of Investigations*. U.S. Bureau of Mines.

Crabtree, D. (1999). BY-PASS EDUCTOR. United States: U.S. Patent Office.

Glenn, R. E., & Craft, B. F. (1986). Air sampling for particulates. Occupational Respiratory Diseases DHHS (NIOSH) Publication, (86-102).

Kissel, F. N. (2003). *Handbook for Dust Control in Mining (IC 9465). Information Circular 9465*. Retrieved from http://www.cdc.gov/niosh/mining/UserFiles/works/pdfs/2003-147.pdf.

Li, T., Salarzar, A. J., & Saito, K. (2009). Experimental and Numerical Feasibility Study of Modifying Automotive Wet Scrubber for Capturing Particulate in Coal-Fired Power Plants. *Sixth International Symposium on Scale Modeling*, 1–10.

McIvor, A., & Johnston, R. (2007). *MINERS’ LUNG* (1st ed.). Burlington, VT: Ashgate.

Manickavasagam, S., & Mengüç, M. P. (1993). Effective optical properties of pulverized coal particles determined from FT-IR spectrometer experiments. *Energy & Fuels*, *7*(6), 860–869. https://doi.org/10.1021/ef00042a023.

Merchant, J., Taylor, G., Hodous, TK. (1986). Coal workers' pneumoconiosis and exposure to other carbonaceous dusts. *Occupational Respiratory Diseases*. (329–400).

MSHA (Mine Safety and Health Administration). (2014). Lowering Miners' Exposure to Respirable Coal Mine Dust, Including Continuous Personal Dust Monitors. *Federal Register*, *79*(84), 24814–24994.

NIOSH (National Institute for Occupational Safety and Health). (1995). *Criteria for a recommended standard: Occupational exposure to coal mine dust*. Washington, DC.

NIOSH (National Institute for Occupational Safety and Health). (2008). *Work-Related Lung Disease Surveillance Report 2007*. Cincinnati, OH.

Public Law 91-173. Federal Coal Mine Health and Safety Act of 1969, Pub. L. No. 30 (1969). 30 USC.

Salazar, A. J. (2012). FLUID SCRUBBER AND SPRAY BOOTH INCLUDING THE FLUID SCRUBBER. United States: U.S. Patent Office.

Sapko, M. J., Cashdollar, K. L., Green, G. M., & Verakis, H. C. (2007). Coal Dust Particle Size Survey of U . S . Mines. *Journal of Loss Prevention Process in the Industries*, *20*(4), 616–620.

U.S. Environmental Protection Agency (U.S. EPA). (2016). *Quality Assurance Guidance Document 2.12 - Monitoring PM2.5 in Ambient Air Using Designated Reference or Class I Equivalent Methods*.

Wilde, F.D., ed., 2006, Collection of water samples (version 2.0, September 2006): U.S. Geological Survey Techniques of Water-Resources Investigations, book 9, chap. A4, http://water.usgs.gov/owq/FieldManual/chapter4/html/Ch4_contents.html.

WHO. (1999). Hazard prevention and control in the work environment: Airborne dust. *Who/Sde/Oeh/99.14*, 1–96. Retrieved from http://www.who.int/occupational_health/publications/en/oehairbornedust3.pdf.

Vita

Adam Joseph Levy graduated from Edwardsville High School in 2010 and enrolled at the University of Kentucky (UK). He graduated from UK in 2015, receiving a Bachelor of Science in Mining Engineering. During his time at UK, Adam held three internships in the coal industry, and worked as a Graduate Research Assistant for Dr. William C. Wedding while pursuing his graduate education. He was a student member of the Society of Mining, Metallurgy, and Exploration.

Adam Joseph Levy